

# Cosmic ray acceleration in supernova remnants

E. G. Berezhko, V. K. Elshin, and L. T. Ksenofontov

*Institute for Space Physics Studies and Aeronomy, Siberian Branch, Russian Academy of Sciences,  
677891 Yakutsk, Russia*

(Submitted 12 May 1995)

Zh. Éksp. Teor. Fiz. **109**, 3–43 (January 1996)

We study the regular acceleration of cosmic rays by shock waves from supernova explosions, based on a simultaneous numerical solution of the diffusive transport equation for the cosmic rays and the equations of gas dynamics. Typical supernova parameters are assumed: explosion energy  $10^{51}$  erg, and initial velocity 4600 km/s of the ejected shell. We assume a Bohm diffusion coefficient for the cosmic rays, and a homogeneous interstellar medium. Cosmic ray acceleration is investigated over the broad range of parameters of the interstellar medium found in the Galaxy. Our numerical results suggest that acceleration is highly efficient—that cosmic rays accelerated by the supernova shock wave account for more than 50% of the energy of the explosion. At the same time, the shock itself does not wind up being completely altered (smooth): the shock always exhibits mixed structure consisting of a thermal front (explosion) and a smooth, extended preshock attributable to cosmic-ray pressure. In the absence of dissipative processes in the preshock region, the overall compression of matter in the shock is an unbounded function of the Mach number ( $\sigma \propto M^{3/4}$ ), and can exceed the factor-of-4 compression in a strong shock with no cosmic rays by more than an order of magnitude. The existence of an efficient mechanism to heat the medium in the preshock region will reduce the degree of compression  $\sigma$  significantly. When the medium is heated by the dissipation of Alfvén waves, the compression is at most a factor of 8. The theory satisfactorily reproduces both the observed cosmic ray spectrum and chemical abundances at energies up to  $\sim 10^{15}$  eV.

© 1996 American Institute of Physics. [S1063-7761(96)00101-1]

## 1. INTRODUCTION

The notion that most observed cosmic rays are produced in supernova explosions was based for a long time on energy considerations (see, e.g., Ref. 1): supernovae are essentially the only class of objects in the Galaxy capable of delivering the requisite power ( $\sim 10^{42}$  erg/s) to the interstellar medium. More recently, this idea has evolved significantly, with the establishment of an efficient cosmic-ray acceleration that can transmit the requisite fraction ( $\sim 10^{41}$  erg/s) of a supernova's explosion energy to cosmic rays.<sup>2,3</sup> From the outset, the high acceleration and universal power-law behavior of the energy spectrum of the accelerated particles, with  $n(\epsilon) \propto \epsilon^{-\gamma}$  ( $\gamma \approx 2$ ), has argued persuasively that regular acceleration plays a dominant role in supernova remnants,<sup>4–7</sup> as these are the very properties required of the cosmic-ray production process to explain both the observed cosmic-ray spectrum and the radio features of supernova remnants.

The spectral hardness of cosmic rays accelerated by a strong shock and their rapid acceleration explain why they become an important dynamic factor that significantly affects shock front structure soon after the onset of acceleration. This back influence of cosmic rays results in substantial thickening of the shock front: apart from the usual thermal front, a shock altered in this way acquires a smooth part—a preshock. The greater the energy invested in cosmic rays, the greater the relative amplitude contributed by the preshock at the expense of the thermal shock. At high enough Mach numbers ( $M \geq 10$ ), the shock is completely altered by cosmic-ray pressure, the thermal shock vanishes, the post-shock gas becomes cold, and all of the free energy in the

shock wave is transmitted by means of cosmic rays.<sup>8–10</sup> This fundamental property of a collisionless shock shows up not only in a steady plane wave,<sup>8</sup> but in the evolving, spherically expanding shock of a supernova in the homogeneous interstellar medium.<sup>11,12</sup>

Note, however, that the evolution of a spherical shock has been studied using a simplified theory in which results obtained in the plane-wave approximation play a central role. Above all, this bears upon the mean cosmic-ray diffusion coefficient, which in the two-fluid (gas + cosmic rays) hydrodynamic description is a parameter that cannot be determined solely within the confines of that theory. It was not previously obvious, however, which features of a plane shock, if any, might show up in a nonsteady shock of finite dimensions. The systematic resolution of this problem requires that one self-consistently determine both the cosmic ray distribution function and the parameters of the gas.

The resultant spectrum of cosmic rays produced by the supernova shock as it evolves is one of the fundamental characteristics of the cosmic ray acceleration process, and it provides a basis for determining the acceleration efficiency—the fraction of the energy liberated in the supernova explosion that is transferred to cosmic rays. This, plus two other important aspects of the acceleration process—the shape of the cosmic-ray energy spectrum and the maximum cosmic-ray energy—cannot be properly handled by simplified approaches in which cosmic rays are treated as a fluid characterized by some energy density and pressure.

Thus, a number of important characteristics of the cosmic-ray acceleration process in supernova remnants can

only be deduced on the basis of a kinetic description, which in turn can only be fleshed out numerically. Kang and Jones<sup>13</sup> were the first to implement such an approach, which they based on the simultaneous numerical solution of the diffusive transport equation for cosmic rays and the gas-dynamic equations. Their theory was limited in scope, however, to the case of weakly energy-dependent cosmic-ray diffusion coefficients ( $\kappa \propto p^\alpha$ ,  $\alpha \leq 0.25$ ). Their work thereby missed the case of greatest physical interest, with a Bohm diffusion coefficient  $\kappa \propto p$ , for which the acceleration efficiency, and consequently the dynamical role played by cosmic rays, is much higher than for a weakly energy-dependent diffusion coefficient.

In essentially the same setting, we have worked out an alternative theoretical description, based on more efficient methods, that makes it possible to study cosmic ray acceleration induced by a supernova shock for an arbitrary function  $\kappa(p)$ .<sup>14</sup> Even our initial investigations disclosed a number of significant differences in the acceleration process, both from the predictions of the plane-wave model, and from results obtained with a simplified approach to the evolution of a spherical shock. Given a Bohm cosmic-ray diffusion coefficient, kinetic theory reproduces the high acceleration efficiency. Moreover, the shock wave does not wind up being completely altered. In fact, as we show below, the nonstationarity of the expanding shock wave and its finite dimensions exert a significant influence on the acceleration of cosmic rays.

In the present paper, we present the results of a systematic study of cosmic-ray acceleration by a spherical shock from a supernova, based on the simultaneous numerical solution of the diffusive transport equation for cosmic rays and the equations of gas dynamics.

## 2. METHOD

The kinetic description of the acceleration and propagation of cosmic rays is based on the diffusive transport equation<sup>15,16</sup> for their distribution function  $f(r, p, t)$ :

$$\frac{\partial f}{\partial t} = \frac{1}{r^2} \frac{\partial}{\partial r} r^2 \kappa \frac{\partial f}{\partial r} - w \frac{\partial f}{\partial r} + \frac{1}{r^2} \frac{\partial}{\partial r} (r^2 w) \frac{p}{3} \frac{\partial f}{\partial p} + Q, \quad (1)$$

in which  $\kappa$  is the cosmic-ray diffusion constant,  $w$  is the velocity of the medium (gas), and the source  $Q$  accounts for the injection of suprathermal particles into the acceleration process.

The medium (gas) is described by the gas-dynamic equations

$$\frac{\partial \rho}{\partial t} + \frac{1}{r^2} \frac{\partial}{\partial r} (r^2 \rho w) = 0, \quad (2)$$

$$\rho \frac{\partial w}{\partial t} + \rho w \frac{\partial w}{\partial r} = - \frac{\partial}{\partial r} (P_g + P_c), \quad (3)$$

$$\frac{\partial P_g}{\partial t} + w \frac{\partial P_g}{\partial r} + \frac{\gamma_g}{r^2} \frac{\partial}{\partial r} (r^2 w) P_g = 0, \quad (4)$$

in which  $\rho$ ,  $w$ ,  $P_g$ , and  $\gamma_g$  are, respectively, the density, velocity, pressure, and adiabatic index of the gas,

$$P_c = \frac{4\pi c}{3} \int_0^\infty dp \frac{p^4 f}{\sqrt{p^2 + m^2 c^2}} \quad (5)$$

is the cosmic-ray pressure,  $m$  is the proton mass, and  $c$  is the speed of light. From here on, unless otherwise noted, the term *cosmic rays* denotes *protons*, the principal ionic constituents of the cosmic medium. Electrons do not play a role in the dynamics, even when they are efficiently accelerated.

We describe the dynamics of the explosively ejected shell in simplified form: we assume that all ejected matter moves at a common velocity  $V_p$ , and that its thermal energy is small compared with the kinetic energy of bulk motion. The motion of the shell (piston) is then governed by the simple equation

$$M_{ej} \frac{dV_p}{dt} = -4\pi R_p^2 [P(R_p + 0) - P(R_p - 0)], \quad (6)$$

where  $M_{ej}$  is the mass of the ejected shell,  $R_p$  is the radius of its outer surface, and  $P = P_g + P_c$  is the total pressure of gas and cosmic rays. The piston is slowed down by the pressure  $P(R_p + 0)$ , transferring its energy to the ambient medium. In this approach, we ignore the reverse shock propagating back into the piston. Nevertheless, the model correctly reproduces the basic global properties of the expanding shell (see, e.g., Refs. 11, 12, and 17).

What we mean by the size (radius)  $R_s$  of the shock is the location of the thermal shock, which for simplicity we take to be a discontinuity. With regard to the gas, the thermal shock possesses all the usual properties of a shock front. Thus, the gas parameters immediately in front of and behind the thermal shock transition region are related by the Rankine–Hugoniot jump conditions:

$$\rho_2 u_2 = \rho_1 u_1, \quad (7)$$

$$\rho_2 u_2^2 + P_{g2} = \rho_1 u_1^2 + P_{g1}, \quad (8)$$

$$\frac{\rho_2 u_2^3}{2} + \frac{\gamma_g}{\gamma_g - 1} u_2 P_{g2} = \frac{\rho_1 u_1^3}{2} + \frac{\gamma_g}{\gamma_g - 1} u_1 P_{g1} - F_{inj}. \quad (9)$$

In these (and subsequent) relations, subscripts 1 and 2 refer to the regions immediately ahead of or behind the thermal shock, respectively,  $F_{inj}$  is the energy flux carried off from the gas in region 2 by a small contingent of the most energetic particles, which are injected during regular acceleration, and  $u = V_s - w$  is the gas velocity relative to the shock front.

Cosmic ray and gas particles could be described by a common distribution function if it were possible to invoke a detailed theory of thermal shock formation. In other words, splitting the resultant particle energy spectrum into gas and cosmic ray components is somewhat arbitrary. But since no such detailed theory presently exists, the separation is necessary, as the gas and cosmic rays are governed by different equations. In our opinion, existing self-consistent models<sup>18–20</sup> describing gas and cosmic ray particles in terms of a common distribution function are inadequately grounded in physics when it comes to dealing with the structure of the thermal shock and particle injection into the acceleration regime.

As usual, we assume cosmic rays to be fast particles whose dynamics, in contrast to gas particle dynamics, require that we allow for diffusion induced by scattering from magnetic field irregularities. We can therefore define an energy  $\varepsilon_{\text{inj}}$  separating gas particles from cosmic rays in the hypothetical common distribution: this is the minimum energy at which  $\lambda$ , the mean free path of scattered particles, exceeds the minimum spatial scale length  $l_{\text{min}}$  of the system. In the present case  $l_{\text{min}}$  is the thickness of the thermal shock. For cosmic ray particles with energy  $\varepsilon > \varepsilon_{\text{inj}}$ , the mean free path  $\lambda > l_{\text{min}}$ , and the thermal shock is effectively a discontinuity. Consequently, the cosmic ray number density is everywhere discontinuous, including at the thermal shock.

The first angular moment of the distribution function, which determines the cosmic ray flux, has a discontinuity at the thermal shock front,

$$\left[ -\kappa \frac{\partial f}{\partial r} - \frac{u}{3} p \frac{\partial f}{\partial p} \right]_1 = Q_0, \quad (10)$$

since the injection of suprathermal gas particles into the acceleration regime is described by the source

$$Q = Q_0 \delta(r - R_s),$$

which is concentrated about the thermal shock. In Eq. (10), we use the notation  $[x]_1^2 = x_2 - x_1$ .

An analysis of measurements carried out near interplanetary shock fronts<sup>21</sup> and numerical modeling of collisionless shocks<sup>22</sup> show that regular acceleration involves a small fraction ( $\sim 10^{-2} - 10^{-3}$ ) of the fastest gas particles. This implies that the energy of the injected particles is a few times the characteristic thermal energy in the shock region. The particle spectrum falls off rapidly at such energies, so the injected particles can be assumed to be monoenergetic:

$$Q_0(p) = \frac{N_{\text{inj}} u_1}{4\pi p_{\text{inj}}^2} \delta(p - p_{\text{inj}}). \quad (11)$$

As noted above, we presently lack any systematic theory enabling us to calculate the number of injected particles  $N_{\text{inj}}$  or their energy  $\varepsilon_{\text{inj}} = p_{\text{inj}}^2 / 2m$ . It is therefore of interest to understand the extent to which the injection rate, which is governed by  $N_{\text{inj}}$  and  $p_{\text{inj}}$ , affects the acceleration of cosmic rays with their attendant consequences. To do so, we can conveniently parametrize these quantities by means of the relations<sup>10,14</sup>

$$N_{\text{inj}} = \eta \rho_1 / m, \quad p_{\text{inj}} = \lambda m c_{s2}, \quad (12)$$

which show that a fraction  $\eta < 1$  of the gas particles crossing the thermal shock is injected, and that the velocity of the injected particles is  $\lambda > 1$  times the speed of sound  $c_{s2}$  in the post-shock region.

Equations (11) and (12) enable one to determine the energy flux in Eq. (9) carried away from the gas by injected particles:

$$F_{\text{inj}} = \eta \frac{\lambda^2}{2} \rho_1 u_1 c_{s2}^2. \quad (13)$$

We restrict our attention here to the case in which the interstellar medium through which the supernova shock

propagates is uniform. Furthermore, for the sake of simplicity, we neglect in our calculations the presence of background cosmic rays in the undisturbed interstellar medium—as we show below, with an expected injection rate of  $\eta \sim 10^{-3}$ , the supernova shock produces far more cosmic rays than would be produced solely by acceleration of Galactic cosmic rays already present in the interstellar medium.

The conditions cited are boundary conditions for Eqs. (1)–(4), and can be written in the form

$$\rho = \rho_0, \quad P_g = P_{g0}, \quad w = 0, \quad f = 0(r \rightarrow \infty). \quad (14)$$

The simplest boundary condition for cosmic rays at the surface of the piston,

$$\frac{\partial f}{\partial r} = 0 \quad (r = R_p), \quad (15)$$

corresponds to assuming that the piston is completely impenetrable to cosmic rays, since the quantity  $-\kappa \partial f / \partial r$  evaluated at the point  $R_p + 0$  determines the cosmic ray flux through the surface of the piston. The pressure  $P(R_p - 0)$  in the equation of motion for the piston then vanishes. When the ambient medium exerts external pressure  $P(R_p + 0)$ , the piston is damped, and it comes to a halt at some time  $t_p$ . Subsequent motion of the piston can be neglected ( $V_p = 0$  at  $t > t_p$ ).

Equation (15) makes physical sense for two reasons. At earlier evolutionary times the matter in the piston is dense, so cosmic ray diffusion within it can be neglected. At later stages of evolution, cosmic ray penetration of the piston can be neglected for another reason: the volume of the piston is much less than the volume bounded by the shock. Below, we quantitatively assess the role played by cosmic ray penetration of the piston, based on calculations that take advantage of this circumstance.

In practice, we can reformulate<sup>14</sup> the boundary condition (10) for the cosmic ray distribution function at the shock front by expressing the term  $(\kappa \partial f / \partial r)_1$  in integral form. To do so, we integrate the transport equation (1) term by term over  $r^2 dr$  from  $R_s + 0$  to  $\infty$ , which yields<sup>14,23</sup>

$$p \frac{\partial f_R}{\partial p} = -\frac{3}{u_p - u_2} \left[ \left[ u_p + \frac{1}{3} \frac{du_p}{d \ln p} + \left( \frac{d}{dt} \int_{R_s}^{\infty} r^2 dr f \right) \frac{1}{R_s^2 f_R} \right] f_R + \left( \kappa \frac{\partial f}{\partial r} \right)_2 - Q_0 \right], \quad (16)$$

where  $f_R(p, t) = f(r = R_s, p, t)$ ,

$$u_p = u_1 - \left( \int_{R_s+0}^{\infty} dr \frac{d}{dr} (r^2 w) f \right) \frac{1}{R_s^2 f_R} \quad (17)$$

is the effective velocity of the medium, which is “sensed” by cosmic rays with momentum  $p$ .

The main difficulty in numerically solving for the evolution of the supernova shock comes in solving the transport equation (1) in the preshock region  $r > R_s$ . There, the distribution of cosmic rays is characterized by the spatial scale

$$l(p) = \kappa(p) / V_s,$$

which is known as the diffusion length, and which varies widely when the diffusion constant depends heavily on the momentum. Thus, for  $\kappa \propto p$  the range can be characterized by  $l(p_{\max})/l(p_{\min}) \sim 10^8$ , and it is essentially impossible to describe a system with that wide a spectrum of scales using standard methods.

This problem becomes amenable to solution upon a change of variables<sup>14</sup> and the use of efficient implicit numerical methods. It then becomes possible to accommodate an arbitrary function  $\kappa(p)$ .

In solving the transport equation (1) for cosmic rays in the preshock region  $r > R_s$ , we transform to the new spatial variable

$$x_c = \exp\left(-\frac{r-R_s}{\kappa_0} V_s\right). \quad (18)$$

The central feature of the simplification here is that the cosmic ray distribution function  $f(x_c, p, t)$  is essentially a linear function (of  $x_c$ ) for all momenta  $p$  and times  $t$ .

An analogous problem arises in solving the gas-dynamic equations (2)–(4) for  $r \geq R_s$ . The functions  $w(r)$  and  $\rho(r)$  given by the cosmic-ray pressure profile  $P_c(r)$  are complicated, and it is essentially impossible to reconstruct them on a uniform grid with the usual spatial variable  $r$ . This problem can be solved in like manner, with a suitable change of spatial variable.

The choice of new variable is based on the following considerations. At  $r > R_s$ , the cosmic-ray pressure for a strong but largely unaltered shock ( $f_R \propto p^{-4}$ ), allowing only for relativistic cosmic rays ( $p > mc$ ), is  $P_c(r) \propto \ln(p_m/p(r))$ , where  $p(r)$  is the minimum momentum of cosmic rays capable of reaching a point at  $r > R_s$ . This quantity can be obtained from the relation

$$\kappa[p(r)]/V_s = r - R_s.$$

Then when  $\kappa \propto p$ , the cosmic-ray pressure can be approximated in the form

$$P_c(r) \propto -\ln\left(\frac{r-R_s}{l_g} + 1\right) + C.$$

The constant  $C$  can be determined by requiring that the cosmic-ray pressure be negligible at some distance  $r_{\max} > R_s$ , so that we can set  $P_c(r_{\max}) = 0$ . The parameter  $l_g$  accounts for the fact that the cosmic-ray pressure varies only slightly at small distances less than the diffusion length of relativistic particles ( $r - R_s < \kappa(mc)/V_s$ ), since relativistic cosmic rays make a small contribution to the pressure.

Therefore, as the new spatial variable to be used in solving the gas-dynamic equations (2)–(4) at  $r > R_s$ , we can choose

$$x_g = \ln\left(\frac{r-R_s}{l_g} + 1\right) \frac{1}{D}, \quad (19)$$

where  $D = \ln[(r_{\max} - R_s)/l_g + 1]$ . Here  $r_{\max}$  and  $l_g$  are chosen in the course of the numerical computations, with  $r_{\max} - R_s$  being several times the maximum cosmic-ray diffusion length. To order of magnitude,  $l_g$  is the same as the diffusion length of particles with momentum  $p = mc$ . In our calculations,

we have taken  $r_{\max} = 1.5R_s$  and  $l_g = 0.3l(mc)$ , thereby satisfying the foregoing requirements and yielding acceptable precision.

As we shall demonstrate below, the functions  $w(x_g)$ ,  $\rho(x_g)$ , and  $P_c(x_g)$  are essentially linear, which significantly facilitates the calculations.

As in our previous paper,<sup>14</sup> we restrict attention to the case of greatest physical interest, with a so-called Bohm diffusion constant

$$\kappa = \rho_B c/3, \quad (20)$$

corresponding to a maximally disturbed (turbulent) medium in which the mean free path  $\lambda$  of cosmic rays prior to scattering equals the gyroradius  $\rho_B$ . Magnetohydrodynamic turbulence (in the guise of Alfvén waves) is efficiently generated by the cosmic rays themselves in the preshock region.<sup>24</sup> An analysis of measurements made near a bow shock<sup>21</sup> and other calculations<sup>21,25</sup> suggest that regular acceleration is accompanied by intense pumping of Alfvén waves, whose amplitudes  $\delta B$  can be comparable to the value  $B$  of the regular magnetic field. In the quasilinear theory, we can formally obtain even higher amplitudes  $\delta B > B$ ,<sup>25</sup> which suggests the necessity of examining nonlinear wave interactions. Although there is presently no corresponding detailed theory, the widely assumed existence of a Bohm diffusion constant (20) near the shock front is based on the supposition that intense pumping of Alfvén waves and nonlinear interactions among them result in the creation of a highly turbulent medium in which  $\lambda \approx \rho_B$ .

Note that at nonrelativistic energies, the diffusion constant (20) differs from the pure Bohm constant  $\rho_B v/3$ . This difference turns out to be completely negligible, however, inasmuch as the typical acceleration time in either case is much less than the typical age of the system (the shock wave).

In addition, we will assume that in a disturbed region, the diffusion coefficient is inversely proportional to the density  $\rho$  of the medium:

$$\kappa = \kappa_0 \rho_0 / \rho, \quad (21)$$

where  $\kappa_0$  depends on the magnetic field  $B_0$  in the undisturbed interstellar medium in accordance with Eq. (20). On the one hand, it stands to reason that compression of the disturbed medium is accompanied by an increase in the magnitude of the chaotic component of the magnetic field  $\delta B$ . At the same time, a diffusion coefficient of the form (21) precludes the development of instability in the preshock region.<sup>26–28</sup> Although the development of large-scale disturbances in that region is indeed a real physical process that can exert a significant influence on cosmic-ray dynamics,<sup>28</sup> we confine our present discussion to the case described by (21) in order to avoid a multitude of complications.

As we have previously described methods of solving (1)–(17) numerically,<sup>14</sup> we forgo such a description here.

### 3. RESULTS

We assume typical values of the supernova explosion energy  $E_{SN} = M_{ej} V_{p0}^2/2$  and initial velocity  $V_{p0}$ :

TABLE I. Parameters of the principal phases of the galactic interstellar medium.

	$N_H,$ $\text{cm}^{-3}$	$\rho_0,$ $\text{g}\cdot\text{cm}^{-3}$	$T_0,$ K	$P_{g0}$	
Hot interstellar medium	0.003	$7.52 \times 10^{-27}$	$10^6$	$1.5 \times 10^{-12}$	
Warm interstellar medium	0.3	$7.52 \times 10^{-25}$	$10^4$	$1.5 \times 10^{-12}$	
	$B_0,$ $\mu\text{G}$	$\kappa_0(mc)$ $\text{cm}\cdot\text{s}^{-1}$	$M_0$	$R_0,$ pc	$t_0,$ $10^3$ yr.
Hot interstellar medium	3	$1.04 \times 10^{22}$	33	22.2	4.72
Warm interstellar medium	30	$1.04 \times 10^{21}$	330	10.3	2.12

$$E_{SN} = 10^{51} \text{ erg}, V_{p0} = 4600 \text{ km/s.}$$

Table I lists the parameters of the so-called hot and warm phases of the interstellar medium through which the disturbance propagates, and which fill most of the Galaxy (see, e.g., Ref. 29). These parameters are the number density  $N_H$  of hydrogen nuclei, the temperature  $T_0$ , and the magnetic field  $B_0$ . The scaling parameters of a spherical shock are determined by the values of these parameters and those of the supernova. Specifically,

$\rho_0 = 1.4N_H m$  is the density of the interstellar medium, assuming the concentration of helium nuclei to be  $N_{\text{He}} = 0.1N_H$ ;

$R_0 = (3M_{ej}/4\pi\rho_0)^{1/3}$  is the radius of the shell at the end of the free expansion stage;

$t_0 = R_0/V_{p0}$  is the duration of the free expansion stage;

$P_0 = \rho_0/V_{p0}^2$  is the dynamical pressure;

$M_0 = V_{s0}/c_{s0}$  is the initial Mach number;

$\kappa_0(mc) = mc^3/3eB_0$  is the diffusion coefficient for a proton with momentum  $p = mc$ .

Apart from the two phases of the interstellar medium noted above, we have carried out calculations for other parameters. Although these other cases do not play nearly so important a role in the Galaxy, considering them enables us to investigate the extent to which the cosmic ray acceleration process is sensitive to the properties of the interstellar medium. We will assume that all of the phases of the interstellar medium that we consider can be approximated by a single

gas pressure  $P_{g0}$  that holds across the Galaxy. We also assume that the magnetic field and density of the medium are related by  $B_0 \propto \sqrt{\rho_0}$ .

The principal factor that governs the level (rate) of injection is the flux of energy carried off from the gas by injected particles at the thermal shock. From Eq. (13), we see that this depends directly on two of the dimensionless parameters that we have introduced,  $\eta$  and  $\lambda$ ; for the sake of simplicity we take  $\lambda = 2$  in all of the cases that we consider. The injected energy flux then depends on  $\eta$ , and by varying  $\eta$  we can study the extent to which the properties of the regular cosmic-ray acceleration process in supernova remnants depend on the injection rate.

### 3.1. Cosmic ray spectrum at a shock front

Figure 1 shows the calculated cosmic-ray distribution function at a shock front ( $r = R_s$ ) at five different times in the evolution of a shock expanding into a hot interstellar medium. The lesser cosmic-ray injection rate [ $\eta = 10^{-4}$ , Fig. 1(a)] yields only modest energy transfer to the accelerated particles. The shock therefore winds up being only slightly altered by cosmic ray pressure, and the cosmic ray spectrum is accordingly similar to the spectrum in the linear approximation. In the free expansion stage ( $t < t_0$ ), the distribution function can be accurately described by a pure power law  $f \propto p^{-q}$  with spectral index

$$q = 3\sigma/(\sigma - 1) \quad (22)$$

close to 4, since the degree of compression  $\sigma$  of a strong shock is close to 4, over the full range between the injection momentum  $p_{\text{inj}}$  and the cutoff momentum  $p_m(t)$ . The latter depends on geometric factors,<sup>23</sup> and can be obtained from

$$q \left[ \frac{2+b-(\nu-1)/\nu}{g_1(p_m)} + \frac{b+d}{g_2(p_m)} \right] = 1, \quad (23)$$

in which  $g_i(p) = R_s u_i / \kappa_i(p)$ , ( $i=1,2$ ) are the so-called modulation parameters. Likewise,  $b = d \ln N_{\text{inj}} / d \ln t$  is the time variation of the injection rate;  $\nu = d \ln R_s / d \ln t$  describes the expansion of the shock; and

$$d = \left[ \frac{R_s}{(u_1 - u_2)r^2} \frac{\partial}{\partial r} (r^2 w) \right]_2$$

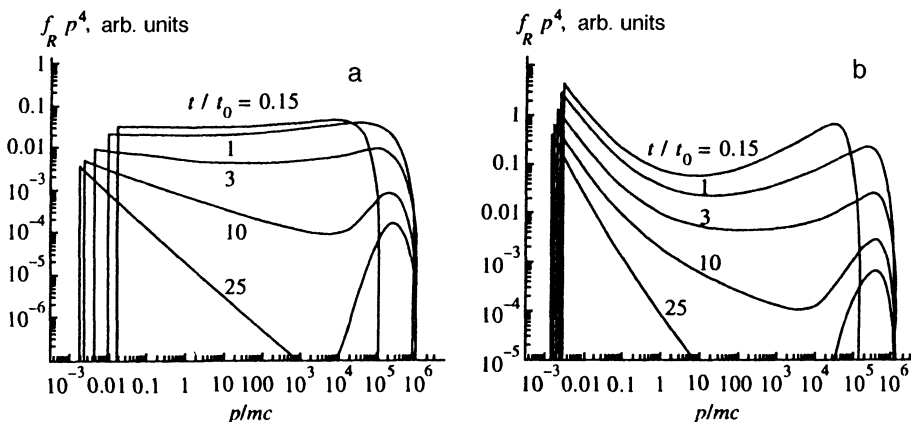


FIG. 1. Cosmic ray distribution function at a shock front as a function of momentum at various times, for an initial Mach number  $M_0 = 33$  and injection rates  $\eta = 10^{-4}$  (a) and  $\eta = 10^{-2}$  (b).

determines the role played by adiabatic variations of cosmic ray energy in the postshock region. Here  $p_m$  is the cosmic ray momentum, where the local spectral index  $d \ln f_R / d \ln p$  is 1 greater than the value of  $q$  given by (22). In a strong shock ( $\sigma=4$ ) with constant injection rate, we obtain a simple expression for the cutoff momentum,

$$p_m(t) = mc \frac{R_s V_s}{K \kappa_0 (mc)}, \quad (24)$$

in which  $K=6$  for the free-expansion stage ( $\nu=1, d=-1/2$ ) and  $K=26$  for the adiabatic stage ( $\nu=2/5, d=3$ ). The cutoff momentum, as can be seen from (24), increases linearly with time in the free expansion stage, which is consistent with the numerical results shown in Fig. 1(a).

At the beginning of the adiabatic stage ( $t > t_0$ ), while the shock is still relatively strong (Mach number  $M \geq 10$ ), the cosmic ray spectrum remains nearly a pure power law  $f \propto p^{-q}$  with a universal spectral index  $q$  (see curves corresponding to times  $t/t_0=1$  and  $t/t_0=3$  in Fig. 1(a)). With time, the shock wave slows down, the Mach number falls, and at  $t/t_0 > 5$ , the compression  $\sigma$  becomes appreciably less than 4. Cosmic rays accelerated by the shock during this time period have a softer spectrum: it is still a power law  $f \propto p^{-q}$ , but the spectral index is much less than 4 and it increases with time as given by Eq. (22) (see curves for  $t/t_0=10$  and  $t/t_0=25$  at  $p/mc \lesssim 10^4$ ).

During this time period, a high-energy component becomes detectable in the cosmic ray spectrum, with dynamics that are fundamentally different from the dynamics of the low-energy part of the cosmic ray spectrum. It is readily apparent in the spectra corresponding to  $t/t_0=10$  and  $t/t_0=25$  in Fig. 1 in the momentum range  $10^4 \lesssim p/mc \lesssim 10^6$ . Against the soft spectral background, this spectral range is dominated at any given time by particles accelerated at the beginning of the adiabatic stage ( $t \sim t_0$ ). During that stage, when they interact relatively weakly with the shock, they are effectively propagating under free diffusion. The volume occupied by these particles has a characteristic size  $R = \sqrt{\kappa_0(p)t}$ . The distribution function in this momentum range therefore varies with time as  $f \propto t^{-3/2}$ . The radius  $R$  varies more rapidly than the size of the shock wave  $R_s \propto t^{2/5}$ . Thus, in a certain sense, these particles can be regarded as escaping: they leave the dynamical region of the system ( $r \leq R_s$ ), carrying off a corresponding fraction of the energy.<sup>28</sup>

Figure 1(b) shows numerical results that differ from the preceding case only in the injection rate: here  $\eta = 10^{-2}$ , two orders of magnitude greater than previously. Due to the high rate of particle injection in the acceleration regime, cosmic rays are an important dynamical factor even at early times (see curve with  $t/t_0=0.15$ ). Their pressure  $P_c$  near the shock front is at least comparable to  $\rho u^2$ . The shock wave is substantially altered by the back influence of cosmic rays on the medium. The shock front is characterized by a total compression  $\sigma \approx 16$ , and consists of a strong preshock and a thermal shock with compression  $\sigma_s \approx 2.5$ . In accordance with (16), the spectrum of cosmic rays accelerated by a weakly modified shock is not a pure power law. If one nevertheless ap-

proximates this with a power law  $f_R \propto p^{-q}$ , then according to (16) the spectral index  $q = -d \ln f / d \ln p$  in the momentum range  $p_{\text{inj}} < p \ll p_m$ , where only the first two terms on the right-hand side are important, will be given by

$$q = \frac{3u_p + du_p / d \ln p}{u_p - u_2}, \quad (25)$$

which can be written in the form

$$q = \frac{3\sigma_p}{\sigma_p - 1} + \frac{d \ln(\sigma_p - 1)}{d \ln p} \quad (26)$$

if we introduce the effective compression  $\sigma_p = u_p / u_2$  "felt" by cosmic ray particles with momentum  $p$ .

Particles with low kinetic energy  $\varepsilon_k < mc^2$  carry a small fraction of the resultant cosmic ray energy, and exert only a minor influence on the structure of the shock front. This means that  $\sigma_p \approx \sigma_s$  for momenta  $p < mc$ . At nonrelativistic energies, therefore, the cosmic ray spectrum is, according to (26), close to a power law with spectral index  $q = q_s \equiv 3\sigma_s / (\sigma_s - 1)$ , the actual value of which depends on the compression  $\sigma_s$  at the thermal shock.

At relativistic energies, the effective velocity of the medium varies from  $u_p = V_s - w_1$  to  $u_p = V_s$  as the momentum ranges from  $p \approx mc$  to  $p \approx p_m$ . The effective compression  $\sigma_p$  is an increasing function of momentum over this energy range, while the spectral index  $q$  decreases. The effective compression varies from  $\sigma_p = \sigma_s$  for particles with momentum  $p \lesssim mc$  to  $\sigma_p = \sigma$  as  $p$  tends to the cutoff momentum.

Several important comments are in order here. First, it is clear from Eq. (26) that the spectral index  $q$  is always greater than  $3\sigma_p / (\sigma_p - 1)$  by virtue of the second term on the right-hand side, which is always positive. The cosmic ray spectrum is therefore always softer than the spectrum given by the linear approximation for a shock with compression factor  $\sigma$ . Even though the effective compression  $\sigma_p$  tends to its full value as the momentum approaches cutoff  $p_m$ , the third and fourth terms in the exact expression (16) become important in this range, leading to softening—and eventually to an abrupt cutoff—of the cosmic ray spectrum. In the case of a strongly modified wave, the spectrum  $p^{-q}$  with spectral index  $q = 3\sigma / (\sigma - 1)$  is never encountered, even locally.

A qualitatively similar cosmic ray spectrum is encountered in the case of a plane shock wave,<sup>30</sup> except that the spectral cutoff in the plane-wave case is due to the finiteness of the acceleration time, rather than the geometrical factors that come into play in the case considered here.

The cosmic-ray spectral features noted here are quite apparent in the behavior of  $f(p)$  in Fig. 1(b) at times  $t/t_0$  of 0.15, 1, and 3, for which the Mach number is still reasonably large. At late times ( $t/t_0=10, t/t_0=25$ ), as before, escaping particles show up in the cosmic ray spectrum.

Figure 2 shows the calculated energy density of accelerated cosmic rays at the shock front ( $r = R_s$ ),

$$\frac{dE_c}{d \ln p} = f_R p^3 \varepsilon_k,$$

for the two injection rates considered above. At the lower rate [Fig. 2(a)], with corresponding minimal alteration of the shock wave, most of the cosmic ray energy is uniformly

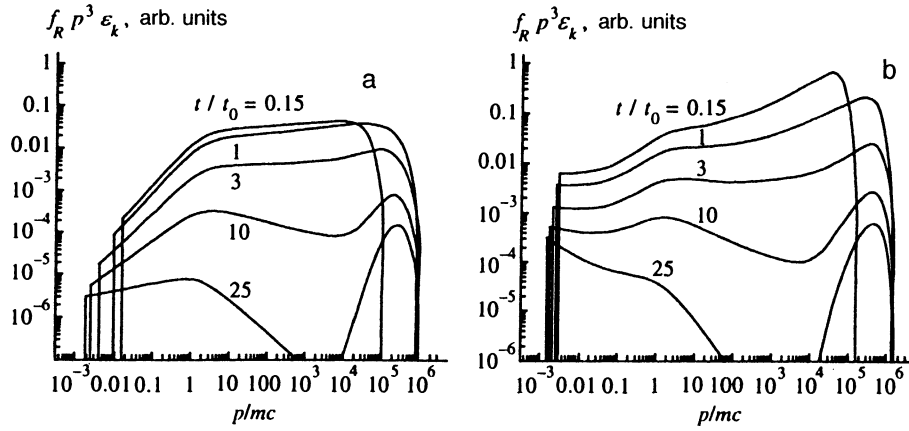


FIG. 2. Cosmic ray energy density (vs.  $\ln p$ ) at a shock front as a function of momentum at various times, for an initial Mach number  $M_0=33$  and injection rates  $\eta=10^{-4}$  (a) and  $\eta=10^{-2}$  (b).

distributed over relativistic energies ( $mc \lesssim p \lesssim p_m$ ) during initial evolution, when the shock is still fairly strong ( $t/t_0 \lesssim 5$ ). As the shock weakens, the energy becomes concentrated near  $p \approx mc$  and  $p \approx p_m$  (escaping particles), which is apparent from the shape of the curves at  $t/t_0=10$  and  $t/t_0=25$  in Fig. 2(a).

The high injection rate and corresponding strong modification of the shock differ in that due to the substantially harder cosmic ray spectrum, most of the energy in the relativistic range is carried by particles at the highest energy  $p \sim p_m$  [Fig. 2(b)] when the shock has a large Mach number. This is in fact a fundamental feature of a supernova shock wave undergoing evolution involving the ongoing acceleration of cosmic rays.

### 3.2. Resultant cosmic ray spectrum

From the standpoint of the cosmic ray production problem, the resultant spectrum produced by the shock wave is of special interest. It can be calculated by integrating the differential number density of cosmic rays at the corresponding time over all space  $R_p \leq r < \infty$ :

$$N(p, t) = 4\pi p^2 \left[ 4\pi \int_{R_p}^{\infty} dr r^2 a f(r, ap, t) \right]. \quad (27)$$

In this expression, the parameter  $a$  accounts for the assumed relaxation of the disturbed medium toward the mean state of the interstellar medium.<sup>31,32</sup> Strictly speaking, Eq. (27)

makes sense only at late enough stages of evolution, when the shock has become weak (small Mach number  $M \lesssim 3$ ) and no longer accelerates cosmic rays efficiently. But it also makes sense to reconstruct the spectrum  $N(p, t)$  at intermediate times  $t$  in order to understand which evolutionary stages contribute most to the resultant cosmic ray spectrum.

An analysis shows that a variety of assumptions about the nature of the relaxation of the medium lead to essentially the same results.<sup>31</sup> For simplicity, then, we make the simplest one: that the density of the medium disturbed by the shock wave relaxes toward the mean state of the interstellar medium. In the process, since the scales are large, the cosmic ray energy varies adiabatically, yielding

$$a(r, t) = [\rho(r, t) / \rho_0]^{1/3}. \quad (28)$$

The resultant cosmic ray spectra given by Eqs. (27) and (28) for the two injection rates considered earlier are shown in Fig. 3.

At low injection rates, the resultant spectrum of shock-induced cosmic rays (see curve for  $t/t_0=25$  in Fig. 3(a)) is close to a power law  $N \propto p^{-\gamma}$  throughout its evolutionary history; the spectral index is  $\gamma \approx 2$  over a wide range of momenta,  $10^{-3} \lesssim p/mc \lesssim 3 \cdot 10^5$ . An analysis of the temporal evolution of the spectrum  $N(p, t)$  shows that most of the cosmic rays in the resultant spectrum were produced in the initial adiabatic stage ( $t/t_0 \lesssim 3$ ), when the Mach number was still high ( $M \geq 10$ ). The contribution at high momenta

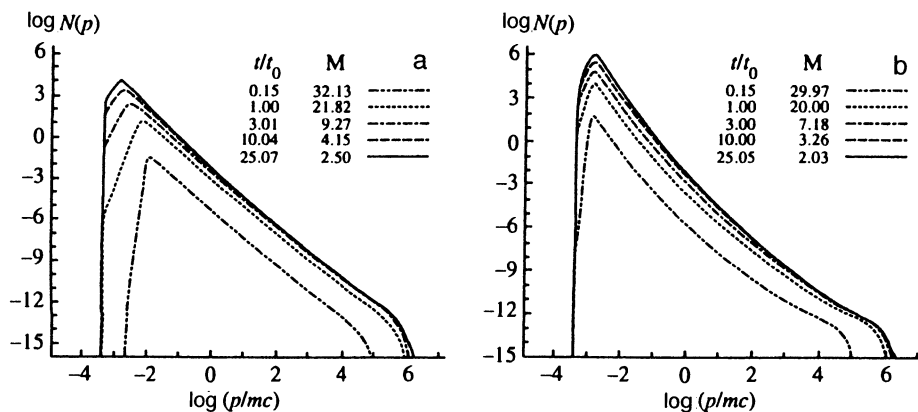


FIG. 3. Resultant spectrum of cosmic rays produced by a shock wave with initial Mach number  $M_0=33$  and injection rates  $\eta=10^{-4}$  (a) and  $\eta=10^{-2}$  (b) at various stage of evolution. ( $N_p$  is measured in relative units).

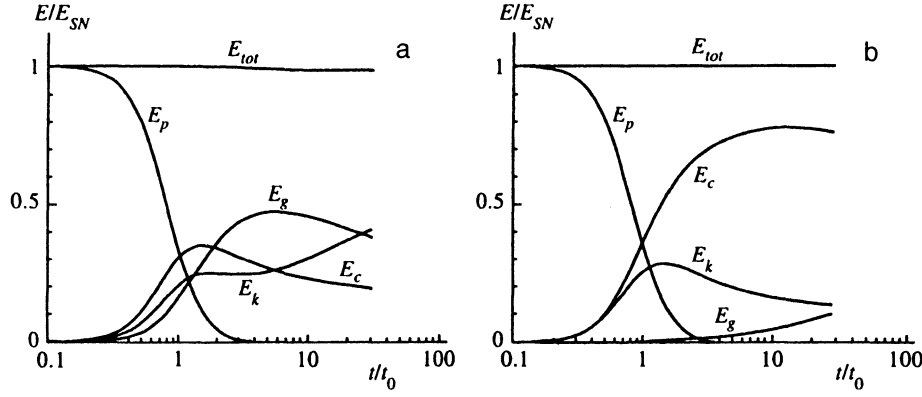


FIG. 4. Time history of piston energy  $E_p$ , cosmic ray energy  $E_c$ , gas kinetic and thermal energy  $E_k$  and  $E_g$ , and total energy  $E_{tot}$  in a shock with initial Mach number  $M_0=33$  and injection rate  $\eta=10^{-4}$  (a) and  $\eta=10^{-2}$  (b).

$p \gg mc$  coming from the later stages, with Mach numbers  $M < 10$ , is negligible.

An analysis of the geometric factors that affect the shape of the spectrum for cosmic rays accelerated by an expanding spherical supernova shock wave shows that the cosmic-ray spectral energy (momentum) peaks at the end of the free expansion stage, with  $p_{max} = \max \{p_m(t)\}$ .<sup>23</sup> We can therefore make use of Eq. (24) to produce an accurate estimate of the maximum cosmic-ray momentum  $p_{max}$ , substituting the appropriate  $R_0$  and  $V_{s0}$  in place of  $R_s$  and  $V_s$ . Taking advantage of the relationship between these parameters, the explosion energy  $E_{SN}$ , and the density  $\rho_0$  of the interstellar medium, as well as (20) and (21) for the cosmic-ray diffusion constant, it is straightforward to obtain a final estimate of the maximum cosmic-ray momentum<sup>23</sup>:

$$\frac{p_{max}}{mc} = 4.43 \cdot 10^5 \left( \frac{E_{SN}}{10^{51} \text{ erg}} \right)^{1/2} \left( \frac{M_{ej}}{10 M_{\odot}} \right)^{-1/6} \times \left( \frac{N_H}{3 \cdot 10^{-3} \text{ cm}^{-3}} \right)^{-1/3} \left( \frac{B_0}{3 \mu G} \right). \quad (29)$$

An accurate calculation for a modest alteration of the shock wave [see Fig. 3(a)] yields  $p_{max}/mc = 4 \cdot 10^5$ , in good agreement with Eq. (29).

The modified shock accelerates high-energy particles more efficiently, so the cosmic-ray spectrum in Fig. 3(a) is harder than previous resultant spectra<sup>31-33</sup> calculated in the linear approximation ( $\gamma=2$  instead of 2.1-2.2).

The spectrum of cosmic rays produced at an injection temperature high enough that the shock wave is appreciably altered [Fig. 3(b)] will no longer be a pure power law in the momentum. The spectrum  $N(p)$  is softer than in the previous case at nonrelativistic energies and low injection rates, and it is harder at relativistic energies. This can easily be understood in light of the most general properties of the acceleration process. At low momenta  $p/mc \sim 10^{-3}$ , the spectral amplitude is directly proportional to the injection rate (i.e., the value of  $\eta$ ). In the second case [Fig. 3(b)], this amplitude is therefore 100 times the amplitude in the first case [Fig. 3(a)]. Hence, it is clear that  $N \propto p^{-2}$  cannot represent some universal spectral behavior when  $\eta=10^{-2}$ , as this would correspond to cosmic ray energies  $E_c$  100 times greater than in the

$\eta=10^{-4}$  case, which is impossible—at  $\eta=10^{-4}$ ,  $E_c$  at late evolutionary stages is more than 20% of the total explosion energy  $E_{SN}$ .

Furthermore, as we have already noted, a substantially modified shock generates a significantly harder cosmic ray spectrum at relativistic energies than an unaltered shock. In other words, for a modified shock, if the cosmic ray spectrum is approximated by a power law  $N \propto p^{-\gamma}$ , the spectral index  $\gamma < 2$  when  $p \gg mc$ , as can be seen in Fig. 3(b). At nonrelativistic energies ( $p < mc$ ), we necessarily have  $\gamma > 2$ . The physical reason for this is that rather than “feeling out” the overall compression, nonrelativistic particles respond solely to the compression  $\sigma_s$  at the thermal shock. In a modified shock,  $\sigma_s$  is less than the compression in an unmodified shock ( $\sigma_s \approx \sigma$  in this case) at the corresponding instant. The alteration of the shock thus results in a softer cosmic ray spectrum at nonrelativistic energies.

Interestingly enough, the maximum momentum  $p_{max} \approx 10^6 mc$  in the resultant cosmic ray spectrum is appreciably higher than in the previous lightly modified shock,<sup>23</sup> because in the present case with  $\eta=10^{-2}$  the total compression reaches  $\sigma \approx 17$ , which is much greater than in the previous case.

### 3.3. System energetics

The different components of the system energy calculated for  $\eta=10^{-4}$  and  $\eta=10^{-2}$  are plotted in Fig. 4. Here

$$E_p = M_{ej} V_p^2 / 2$$

is the kinetic energy of the shell,

$$E_k = 2\pi \int_{R_p}^{\infty} dr r^2 \rho w^2$$

is the kinetic energy of the gas,

$$E_g = 3\pi \int_{R_p}^{\infty} dr r^2 (P_g - P_{g0})$$

is the thermal energy imparted to the gas by the shock,

$$E_c = 4\pi \int_{R_p}^{\infty} dr r^2 \left[ 4\pi \int_0^{\infty} dp p^2 \epsilon_k f \right]$$

is the kinetic energy of cosmic rays, and

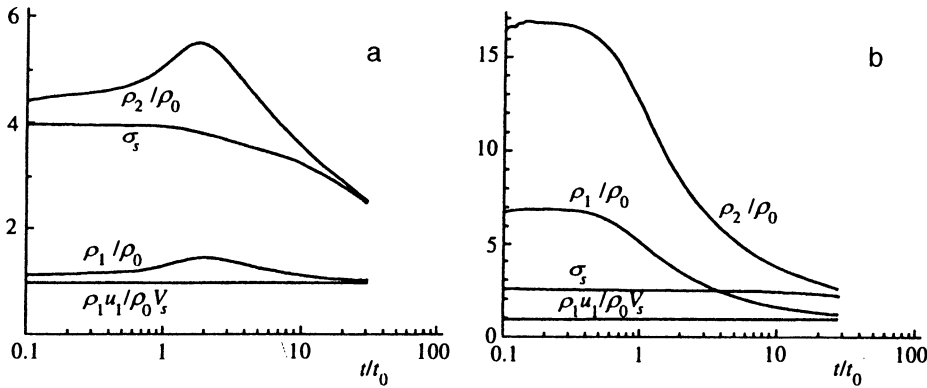


FIG. 5. Time history of total compression  $\rho_2/\rho_0$ , preshock compression  $\rho_1/\rho_0$ , compression at the thermal shock  $\sigma_s$ , and flux density of matter at the thermal shock  $\rho_1 u_1$  for an initial Mach number  $M_0=33$  and injection rate  $\eta=10^{-4}$  (a) and  $\eta=10^{-2}$  (b).

$$E_{\text{tot}} = E_p + E_k + E_g + E_c$$

is the total system energy less the thermal energy of the interstellar medium.

Given the way it has been defined,  $E_{\text{tot}}$  ought to be constant in time and equal to the explosion energy  $E_{SN}$ . Deviations of  $E_{\text{tot}}/E_{SN}$  from unity can only result from computational errors. It is clear from Fig. 4 that this ratio remains within 1% of unity even in the latest stages, a result that we consider to be perfectly satisfactory.

At  $t=0$ , the energy of the system consists entirely of the kinetic energy of the shell (piston) ejected in the explosion. As the piston expands, it transfers energy to the gas and cosmic rays, decelerating in the process. The shape of the function  $E_p(t/t_0)$  is essentially independent of the parameters of the problem, since  $t_0$  in fact defines the characteristic dynamical time constant of the piston.

The cosmic ray energy  $E_c$  at the lesser injection rate [Fig. 4(a)] peaks at  $1 < t/t_0 < 2$ , and then decreases slowly. Although the shock front continues to produce cosmic rays efficiently even at  $t/t_0 \geq 2$ , adiabatic cosmic-ray energy losses in the expanding postshock region ( $r < R_s$ ) begin to dominate. Nevertheless, even when the injection rate is as low as  $\eta = 10^{-4}$ , more than 20% of the total supernova energy  $E_{SN}$  is transferred to cosmic rays. Naturally, as the injection rate rises, so does the energy transferred to cosmic-ray particles: at  $\eta = 10^{-2}$  (Fig. 4(b), cosmic rays carry 80% of  $E_{SN}$ .

### 3.4. Structure of the shock front

Figure 5 shows the temporal evolution of the total compression  $\sigma = \rho_2/\rho_0$ , the preshock compression of matter  $\rho_1/\rho_0$ , the compression at the thermal shock  $\sigma_s = \rho_2/\rho_1$ , and the flux density of matter  $\rho_1 u_1$  at the thermal shock in units of  $\rho_0 V_s$ , all for  $\eta = 10^{-4}$  and  $\eta = 10^{-2}$ . For the same two cases, Fig. 6 shows the velocity of the medium ahead of ( $w_1$ ) and behind ( $w_2$ ) the thermal shock, as well as the cosmic ray pressure  $P_c$  at the shock front.

At the lower injection rate ( $\eta = 10^{-4}$ ), the ratio of the cosmic ray pressure to the dynamical pressure  $\rho_0 V_s^2$  [Fig. 6(a)] increases smoothly with time at first, peaking at  $t/t_0 \approx 2$ . The reason is that for an essentially constant amplitude of the distribution function, the cutoff momentum  $p_m(t)$  rises with time (see Fig. 1). An increase in the cosmic ray pressure is accompanied by an increase in the preshock compression of matter  $\rho_1$ , the total compression  $\sigma = \rho_2/\rho_1$ , and the velocity of the medium ahead of the thermal shock, as can be seen from Figs. 5(a) and 6(a). Later on, at  $t/t_0 > 2$ , all of these quantities are smoothly decreasing. Two factors come into play here: a drop in the Mach number, and a decrease in  $R_s V_s$ , which governs the value of the cutoff momentum for the cosmic rays being accelerated at that time.

At the higher injection rate, the cosmic ray pressure [see Fig. 6(b)] and accordingly  $\sigma$ ,  $\rho_1$  [Fig. 5(b)], and  $w_1$  [Fig. 6(b)] all peak at very early stages in the expansion,

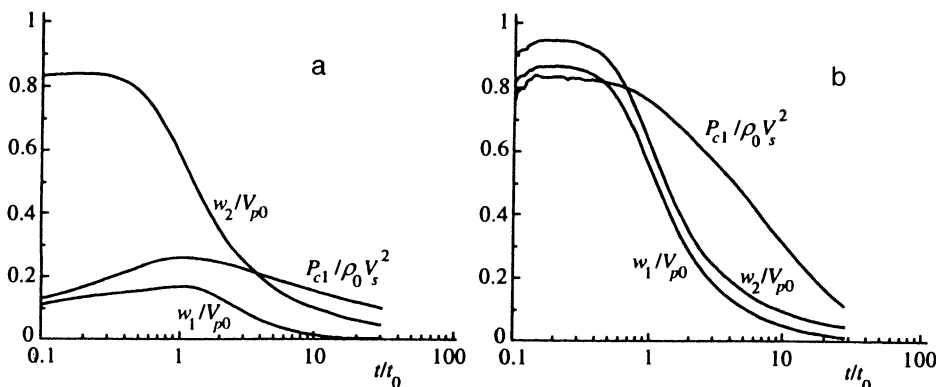


FIG. 6. Time history of the velocity of the medium ahead of ( $w_1$ ) and behind ( $w_2$ ) the thermal shock, and of the cosmic ray pressure at the thermal front, for an initial Mach number  $M_0=33$  and injection rate  $\eta=10^{-4}$  (a) and  $\eta=10^{-2}$  (b).

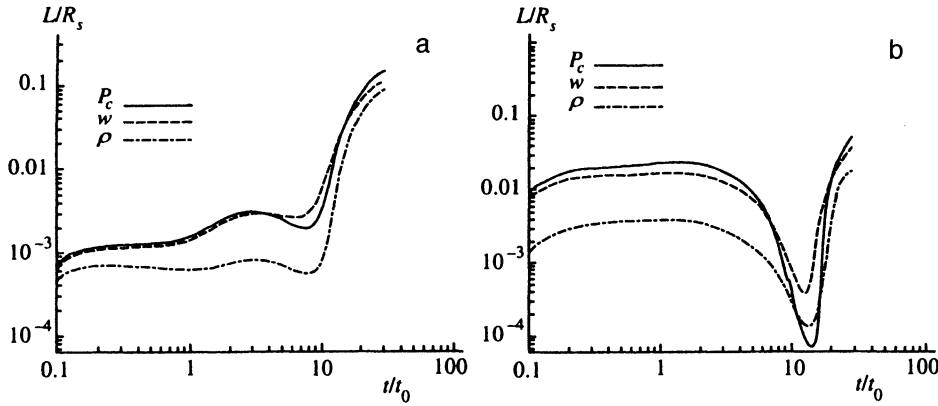


FIG. 7. Scale size of the preshock as a function of time for a shock wave with initial Mach number  $M_0=33$  and injection rate  $\eta=10^{-4}$  (a) and  $\eta=10^{-2}$  (b).

$t/t_0 \approx 0.1$ . The pressure due to cosmic rays is then governed by their self-regulating nonlinear interaction with the medium, and depends only weakly on the value of the cutoff momentum  $p_m(t)$ .

It is noteworthy that the flux density of matter  $\rho_1 u_1$  is close to  $\rho_0 V_s$  in all cases, as in a steady plane shock, where  $\rho u = \rho_0 V_s$  in the preshock region. This is so because the size  $L$  of the preshock is always small compared to the size  $R_s$  of the shock itself.

The width of the preshock can be determined from the relation

$$\frac{X(R_s)}{X(R_s + L)} = e, \quad (30)$$

according to which  $L$  is the distance from the thermal shock at which the value of  $X$  decreases by a factor of  $e$ . Here  $X$  can stand for  $P_c$ ,  $w$ , or  $\rho - \rho_0$ .

Figure 7 shows the value of  $L$  as a function of time, calculated using Eq. (30). At the lower injection rate  $\eta=10^{-4}$ ,  $L/R_s \approx 10^{-3}$  [Fig. 7(a)], except at the very latest stages of expansion  $t/t_0 > 8$ , when it starts to increase rapidly, reaching  $L/R_s = 0.1$  at  $t/t_0 = 20$ . The latter has to do with the influence of escaping particles (see Fig. 1). We have already noted that these are the highest-energy particles in the cosmic ray spectrum, and the linear size of the region that they occupy grows faster than does the size of the shock wave  $R_s$ . Thus, in the later stages of evolution, when the shock is fairly weak and escaping particles become the dominant energy component at  $r > R_s$  (see Fig. 2), the preshock begins to grow rapidly. Of course, it must be borne in mind that the shock is weak at that point, and that the efficiency of cosmic ray acceleration is low.

As the injection rate increases, with concomitantly greater alteration of the shock, the preshock grows as well. It is easy to see why the scale length  $L$  increases as the injection rate rises. With increasing  $\eta$ , the shock becomes further modified, and the cosmic ray spectrum becomes harder and harder (see Fig. 1). The energy in the cosmic ray spectrum becomes more and more concentrated near the cutoff momentum  $p_m(t)$ . This means that in a substantially modified wave, the scale size of the preshock is, to order of magnitude, the same as the diffusion length of particles with momentum  $p_m$ . In conjunction with (24), this yields

$$L \sim R_s / K.$$

Hence, it is clear that the limiting value of  $L/R_s$  is approximately 0.17. At  $\eta=10^{-2}$  [Fig. 7(b)], the preshock width given by  $P_c$  and  $W$  reaches 0.03 during the period of efficient cosmic ray acceleration ( $t/t_0 \lesssim 3$ ), which is still appreciably less than the limiting value.

The local minimum in  $L(t)$  near  $t/t_0 = 10$  results from the energy-bearing component of the cosmic rays at that point being nonrelativistic particles with a short diffusion length (see Fig. 2).

The density distribution  $\rho(r)$  of the preshock medium, as is clear from Fig. 7, has a shorter scale length than the velocity distribution  $w(r)$ , which in turn is similar to the cosmic ray pressure profile  $P_c(r)$ . The reason is that the density and velocity of the medium at  $r > R_s$  are simply related by

$$\rho - \rho_0 = \rho_0 w / u,$$

a consequence of the constancy of the flux density of matter  $\rho u$ . Clearly, then, when  $r > R_s$ ,  $\rho - \rho_0$  decreases faster than  $w$ , since  $u(r)$  then increases as well. The difference in scale lengths  $L$  between the density and flux-density distributions is especially notable in a significantly modified shock.

Figure 8 shows the velocity profile  $w(r)$  at five times for the medium at  $r > R_s$  with  $\eta = 10^{-3}$ . The behavior of  $w(r)$  here is clearly complicated. The characteristic scale length  $L = |w / (dw/dr)|$  is itself a function of distance from the thermal shock, and varies widely. In order to understand the behavior of  $w(r)$ , we analyze Eq. (3), introducing the new spatial variable  $x = R_s - r$  and neglecting the minor terms  $\partial w / \partial t$  and  $\partial P_g / \partial x$ . Noting that  $\rho u = \rho_0 u_0$  at  $r > R_s$ , we obtain the simple equation

$$\rho_0 V_s \frac{\partial w}{\partial x} = \frac{\partial P_c}{\partial x},$$

which shows that the preshock scale lengths of  $w(r)$  and  $P_c(r)$  are the same (as also shown by the results plotted in Fig. 7). The efficacy of the new spatial variable  $x_g$  given by (19) is illustrated by Fig. 9, which shows  $w(x_g)$  at  $r > R_s$  ( $x_g = 0-1$ ). Then  $w(x_g)$  is clearly not that far from being

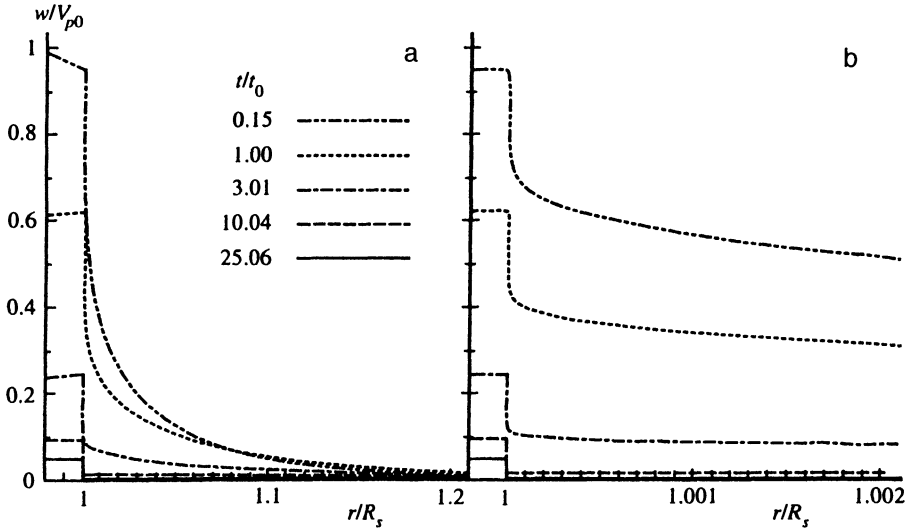


FIG. 8. Velocity profile of the medium for a shock wave with initial Mach number  $M_0=33$  and injection rate  $\eta=10^{-3}$ .

linear, which makes it possible to represent it numerically to high precision with a fairly small number of points (100 at most).

Figure 10 shows the spatial dependence of the cosmic ray distribution function for four values of the energy at four different times ( $\eta=10^{-4}$ ). In the preshock region  $r>R_s$ , there is clearly a quasilinear relationship at all  $p$  and  $t$  between  $\ln f$  and  $r$  and between  $f$  and  $x_c$ , which justifies the choice of variable  $x_c$  at  $r>R_s$ .

### 3.5. Influence of the interstellar medium and injection rate on the efficiency of cosmic ray acceleration

Besides the hot interstellar medium assumed in all of the preceding calculations, other phases of the Galaxy are often invoked—for example, the so-called warm interstellar medium, with  $T_0 \approx 10^4$  K,  $N_H \approx 0.3 \text{ cm}^{-3}$  (see, e.g., Ref. 29). It is therefore of interest to study the evolution of a supernova shock and the acceleration of cosmic rays for a variety of interstellar media. To keep things simple, we assume that all phases of the interstellar medium are at the same pressure,  $P_{g0} = 10^{-12} \text{ dyn/cm}^2$ , which is approximately true of the Galaxy.<sup>29</sup> The different phases of the interstellar medium can

then be distinguished from one another by just one more parameter, such as the temperature  $T_0$ , density  $\rho_0$ , or some combination of the two. A convenient choice that specifies the properties of the interstellar medium is the initial Mach number  $M_0 = V_{s0}/c_{c0}$ , a dimensionless parameter that directly accounts for shock evolution. Since all of the following calculations are carried out for a single initial shock ve-

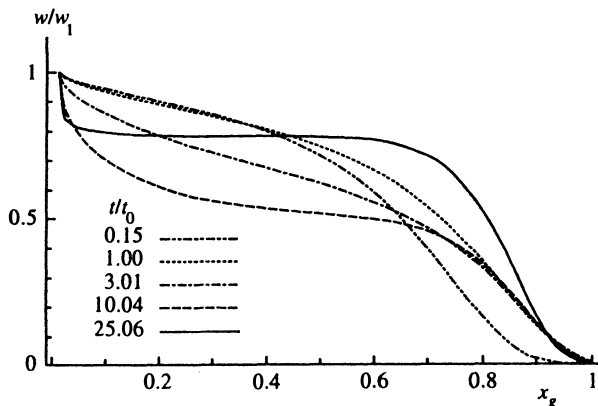


FIG. 9. Same as Fig. 8, but plotted as a function of the new spatial variable  $x_g$  defined by Eq. (19).

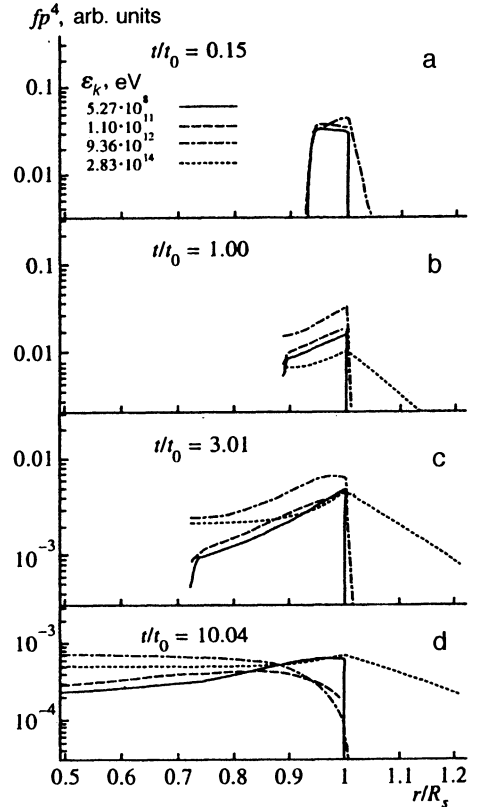


FIG. 10. Cosmic ray distribution function at four different energies and times as a function of distance for an initial Mach number  $M_0=33$  and injection rate  $\eta=10^{-4}$ .

locity  $V_{s0} = 1.1V_{p0}$  ( $V_{p0} = 4600$  km/s), the Mach number should enable us to determine all of the parameters of the interstellar medium.

Finally, we assume that the magnetic field and density of the interstellar medium are related by  $B_0 \propto \sqrt{\rho_0}$ .

Since  $\eta$ , which defines the particle injection rate at the thermal shock in the acceleration regime, is a free parameter in our theory, it makes sense to study the progress of shock evolution and the acceleration of cosmic rays as functions of  $\eta$ .

The amount of information encompassed by the state and evolution of the system under study is enormous, so we limit our scope and discuss just the basic parameters, which above all reflect upon the efficiency of the cosmic ray acceleration process and its influence on shock structure. Among the most useful such parameters are the maximum total cosmic ray energy  $E_c$  attained during evolution, the cosmic ray pressure  $P_c$  at the shock front (relative to the dynamical pressure  $\rho_0 V_s^2$ ), the total compression  $\sigma$ , and the compression at the thermal shock at the same instant. Here the maximum energy  $E_c$  characterizes the efficiency of cosmic ray acceleration, which to good accuracy can be viewed as the total energy committed to cosmic rays throughout the evolution of the shock, since as we showed earlier in a number of examples, the cosmic ray energy  $E_c(t)$  remains essentially constant once it has reached its maximum. Furthermore, the presumed relaxation process in the disturbed medium can also alter (raise) the cosmic ray energy somewhat, making the assessment of the energy transferred to cosmic rays a bit uncertain. We thus conclude that the quantity  $(E_c/E_{SN})_{\max}$  reasonably fully characterizes the efficiency of cosmic ray acceleration. The same can be said of  $\sigma_{\max}$ : it reflects the degree to which the structure of the shock has been modified by cosmic rays.

The quantities plotted in Fig. 11 are shown as a function of the initial Mach number  $M_0$  for four values of the injection rate  $\eta$ , while in Fig. 12 they are shown as a function of the injection rate  $\eta$  for five values of  $M_0$ .

The most notable feature of Fig. 11 is that all of the quantities except  $\sigma$  are rising functions of  $M_0$ , a consequence of the fact that a stronger shock accelerates cosmic rays more efficiently, and is therefore itself more significantly modified by the back influence of the cosmic rays. The compression of matter at the thermal shock,  $\sigma_s$ , then decreases with increasing  $M_0$ , although  $\sigma_s(M_0)$  is a slowly varying function. Under more physically interesting conditions ( $\eta = 10^{-4} - 10^{-3}$  and  $M_0 > 10$ ), the compression  $\sigma_s$  lies in the fairly narrow range 3–4.

In contrast, the total compression  $\sigma$  is a strong function of the Mach number. At any given injection rate, the compression follows a power law,  $\sigma \propto M_0^\alpha$ , with  $\alpha \approx 0.75$  (see Fig. 11).

### 3.6. Critical injection rate

It can be seen from Fig. 12 that there is a big difference in the efficiency of acceleration as a function of injection rate at low and high values of  $\eta$ . The behavior of  $E_c(\eta)$  and  $P_c(\eta)$  and  $(\sigma(\eta))$  as well) is such that there exists for any

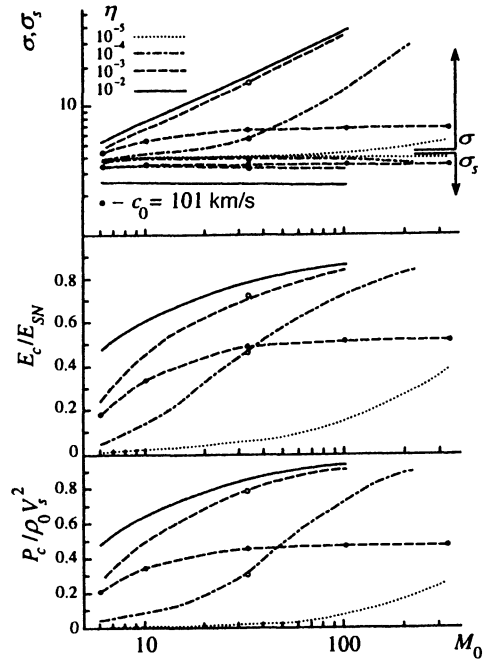


FIG. 11. Cosmic ray compression  $\sigma$ , energy  $E_c$ , and pressure  $P_c$  in units of the dynamical pressure  $\rho_0 V_s^2$  (maximum values attained during evolution) as a function of the initial Mach number  $M_0$ , for various injection rates  $\eta$ . The compression  $\sigma_s$  at the thermal shock is calculated at the same instant as  $\sigma$ . Curves for  $M_0 = 33$  and  $M_0 = 330$  with black dots were computed with Alfvén wave dissipation taken into account. Unfilled dots correspond to  $M_0 = 33$  and  $\eta = 10^{-4}, 10^{-3}$ , with cosmic ray penetration of the piston.

Mach number a critical value  $\eta_*(M_0)$  of  $\eta$  that divides the two substantially different ranges. For the sake of definiteness, let us take for  $\eta_*$  the value of  $\eta$  that makes

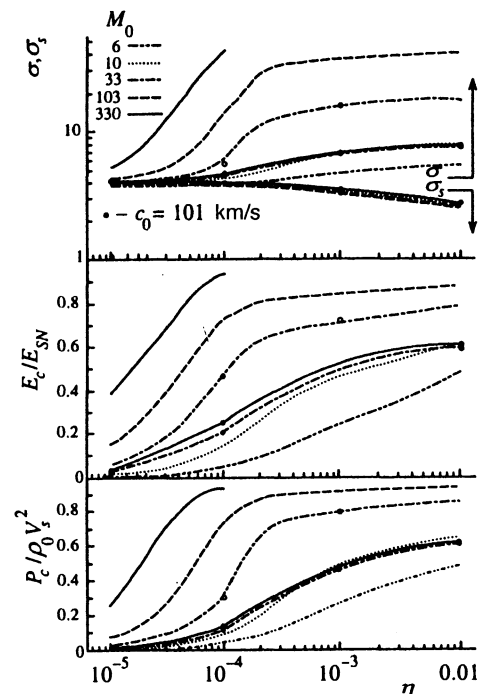


FIG. 12. Same as Fig. 11, but plotted as a function of the injection rate  $\eta$  for various values of the initial Mach number.

$P_c/\rho_0 V_s^2 = 0.1$ . We then find that for  $\eta < \eta_*$ , both  $E_c(\eta)$  and  $P_c(\eta)$  are close to linear, and the total compression of a strong shock is close to 4. Acceleration of cosmic rays with  $\eta < \eta_*$  takes place in the linear regime: by virtue of the low injection rate, the cosmic ray pressure  $P_c$  is low compared to the dynamical pressure  $\rho_0 V_s^2$ , and the shock remains essentially unaltered. This can also be called the unsaturated regime.

We can easily identify the factors that determine the critical injection rate  $\eta_*$ . On the one hand, given the definition of  $\eta_*$ , the cosmic ray pressure at the shock front is  $P_{c*} = 0.1 \rho_0 V_s^2$ . At the same time, we can express this pressure in terms of  $\eta_*$ : we merely note that the cosmic ray distribution function at a largely unmodified shock front conforms to a power law,

$$f = \eta_* \left( \frac{\rho_0}{m} \right) \frac{q}{4\pi p_{\text{inj}}^3} \left( \frac{p}{p_{\text{inj}}} \right)^{-q},$$

with  $q = 4$  and injection momentum  $p_{\text{inj}} \approx m V_s$ . Also bearing in mind that relativistic particles make the major contribution to the pressure, we obtain

$$P_{c*} = \frac{4}{3} \eta_* \rho_0 V_s c \ln \frac{p_m}{mc}, \quad (31)$$

whereupon

$$\eta_* = \frac{3V_s}{40c \ln(p_m/mc)}. \quad (32)$$

Hence, all other things being equal, it is clear that a shock with a lesser velocity  $V_s$  is more easily modified by cosmic ray pressure, or in other words, the lower the velocity  $V_s$ , the fewer the cosmic rays required to produce the same modification. This means that at a constant injection rate, a shock with a high initial Mach number  $M_0 > 10$  will be maximally altered at the instant when its velocity begins to decrease, but it will still remain strong. Assuming that the minimum Mach number for a strong shock is approximately  $M = 10$ , we conclude that we need  $V_s = 10V_{s0}/M_0$  in (31) instead of  $V_s$ , which then yields the final expression for the critical injection rate:

$$\eta_* = \frac{3V_{s0}}{4M_0 c \ln(p_m/mc)}. \quad (33)$$

In the present case  $p_m/mc \approx 4 \cdot 10^5$ ,  $V_{s0} \approx 5000$  km/s, so that  $\eta_* \approx 10^{-3}/M_0$ . At  $M_0 = 33$  (hot interstellar medium) the critical injection rate is  $\eta_* = 3 \cdot 10^{-5}$ , and at  $M_0 = 330$  (warm interstellar medium)  $\eta_* = 3 \cdot 10^{-6}$ . It can easily be shown that the derived value of  $\eta_*$ , and in fact Eq. (33) as a whole, are in good agreement with the results obtained numerically (Fig. 12).

As  $\eta$  increases, with  $\eta > \eta_*$ , the cosmic ray energy and pressure rise rapidly, ultimately becoming weak functions of  $\eta$ . At high enough Mach numbers in this saturated cosmic-ray acceleration regime, large values of  $E_c/E_{SN}$  and  $P_c/\rho_0 V_s^2$  exceeding 0.7 are attained.

Note that the cosmic ray acceleration exhibits similar behavior in the plane-wave approximation if an additional parameter—the cutoff momentum  $p_m$ —is introduced at the

outset, and if one allows for the energy removed from the system by particles that can reach the limiting momentum  $p_m$ .<sup>20,34,35</sup> In the present description, where the finite size of the shock is a natural consideration, there is no need to introduce such a parameter. The cosmic ray spectrum is instantaneously bounded by virtue of geometrical factors.<sup>23</sup> In contrast to a plane shock, the volume occupied by accelerated particles at  $r \geq R_s$ ,  $V \propto R_s^2 \kappa(p)/V_s$ , increases with time due to the growth in  $R_s$  and the decreasing velocity  $V_s$  of the shock. On the other hand, their rate of acceleration falls (the characteristic acceleration time<sup>36,37</sup> is  $\tau \propto V_s^2/\kappa$ ).

We see, then, that when the cosmic ray diffusion coefficient  $\kappa(p)$  rises with momentum, particle acceleration at high  $p$  by a spherical shock is incapable of filling the volume  $V$  with accelerated particles to the same density as in the case of a plane shock. The value of cosmic ray momentum at which geometrical factors become important is given by Eq. (23).

Note that geometrical factors are more important than temporal factors in an expanding shock: the cutoff momentum given by (23) is always less than the limiting momentum attained in a plane shock with the same time dependence of  $V_s$ .<sup>23</sup> This plays an exceptionally important role in dictating the nature of the modification to the shock. It is precisely the geometrical factors that explain why, as shown by the foregoing calculations, an expanding spherical shock is not completely modified by cosmic ray pressure, no matter how high the Mach number.<sup>38</sup> Simplified versions of the theory—for example, a two-fluid (gas plus cosmic rays) hydrodynamic description—can lead to inconsistencies, due to improper allowance for these factors. In the hydrodynamic theory, information on the relationships among spatial scales in the cosmic ray distribution resides in the spectral mean of the diffusion coefficient,  $\bar{\kappa}(r, t)$ . The strong momentum dependence of the initial diffusion coefficient  $\kappa$  inevitably leads to a strong  $r$ -dependence of the mean coefficient  $\bar{\kappa}$  at  $r \geq R_s$ . Since the behavior of  $\kappa(p)$  exercises a decisive influence on the nature of cosmic ray acceleration, a proper hydrodynamic description must incorporate the correct function  $\bar{\kappa}(r)$ . Two-fluid hydrodynamic models presently in use rely on the plane-wave approximation to estimate  $\bar{\kappa}(t)$ , and fail to take account of the  $r$ -dependence of  $\kappa$ .<sup>11,12,39–41</sup>

### 3.7. Compression

There are two aspects to the back influence of cosmic rays on the medium. The transfer of a substantial fraction of the energy of the shock to cosmic ray particles is always accompanied by a rise in the total compression of matter  $\sigma$ . This rise in  $\sigma$ , in turn, makes the acceleration of cosmic rays a more efficient process—the pace of acceleration increases, and the cosmic ray spectrum becomes harder. A positive feedback loop in the nonlinear interaction between cosmic rays and the medium thus ensues.

The system reaches an equilibrium state mediated by a negative feedback loop: modification of the shock is accompanied by a decrease in the compression  $\sigma_s$  of the thermal shock, which, as previously noted, directly affects the shape of the nonrelativistic cosmic ray spectrum. A decrease in

$\sigma_s$  results in softening of the cosmic ray spectrum  $f(p)$  at  $p < mc$ , and in the final analysis precludes any excessive rise in the spectral amplitude in the relativistic range, which carries the brunt of the energy.

In order to understand which factors affect the compression of matter at the thermal shock, we adopt a simplified model of the cosmic ray spectrum at the front of a modified strong shock. This model consists of two pure power laws:

$$f_R = \begin{cases} a \left( \frac{p}{p_{\text{inj}}} \right)^{-q_s} & \text{for } p_{\text{inj}} \leq p \leq mc, \\ a_{mc} \left( \frac{p}{mc} \right)^{-q} & \text{for } mc \leq p \leq p_m, \end{cases}$$

which can be seen from previous calculations (Fig. 1) to provide an adequate approximation. It must also be kept in mind that  $q_s > 4$  and  $3 < q < 4$ . The cosmic ray pressure can be easily calculated based solely on relativistic particles:

$$P_c = \frac{4\pi(mc)^3 a_{mc}}{3(4-q)} \left( \frac{p_m}{mc} \right)^{4-q} (mc)^2.$$

The amplitude  $a_{mc}$  is related to the amplitude at the injection point by

$$a_{mc} = a \left( \frac{mc}{p_{\text{inj}}} \right)^{-q_s}.$$

We can also write the cosmic ray pressure in the form  $P_c = kP_{c*}$ . Since by definition the critical pressure is 10% of the dynamical pressure  $\rho_0 V_s^2$ , we clearly have  $1 < k < 10$ . Writing the critical pressure in the form  $P_{c*} = (4\pi/3)p_{\text{inj}}^4 c a_* \ln(p_m/mc)$  and noting that  $a/a_* = \eta/\eta_*$ , we obtain

$$q_s = 4 + \frac{\ln(\eta/\eta_*)}{\ln(mc/p_{\text{inj}})} + \ln \left[ \left( \frac{p_m}{mc} \right)^{4-q} \frac{1}{(4-q)k \ln(p_m/mc)} \right] \frac{1}{\ln(mc/p_{\text{inj}})}. \quad (34)$$

Noting further that under a substantial modification  $k < 10$ ,  $3 < q < 4$ , and that the typical injection and cutoff momentum are given by  $p_{\text{inj}}/mc \approx 2 \cdot 10^{-3}$  and  $p_m/mc \approx 4 \cdot 10^5$ , it can easily be shown that the third term on the right-hand side of Eq. (34) can be neglected. Bearing in mind that  $q_s = 3\sigma_s/(\sigma_s - 1)$ , we obtain an expression for the compression at the thermal shock,

$$\sigma_s = 1 + \frac{3}{1 + \ln(\eta/\eta_*)/\ln(mc/p_{\text{inj}})}. \quad (35)$$

This expression accounts for the weak (logarithmic) dependence of the preshock compression at the front on the injection  $n > \eta_*$  rate and on the Mach number  $M_0$ , which has been corroborated computationally (see Fig. 11). Direct comparison with the results in Fig. 11 shows that the expression accounts for the quantitative behavior of  $\sigma_s$  if we employ the critical injection rate  $\eta_*$  found above.

On the other hand, if in Eqs. (7)–(9) we ignore the energy flux  $F_{\text{inj}}$  carried by injected particles (which is permis-

sible if the injection rate is not too high), the compression  $\sigma_s = \rho_2/\rho_1$  will be expressible as usual in terms of the local Mach number  $M_1 = u_1/c_{s1}$ :

$$\sigma_s = \frac{4}{1 + 3/M_1^2}. \quad (36)$$

Here  $c_{s1} = \sqrt{5P_{g1}/3\rho_1}$  is the local speed of sound immediately ahead of the thermal shock, and we have taken  $\gamma_g = 5/3$ . A compression of  $\sigma_s = 3$  corresponds to  $M_1 = 3$ .

We can therefore conclude that the distinctive feature of the preshock is that the medium there is compressed to such a degree as to ensure that Eqs. (35) and (36) hold for the Mach number  $M_1$ . It is not difficult to establish the relationship between the preshock compression of matter  $\rho_1/\rho_0$  and the total compression  $\sigma$ , on the one hand, and compression  $\sigma_s$  at the thermal shock, on the other.

It follows from (2) and (4) that at  $r > R_s$ , the gas pressure and density are adiabatically related:

$$P_g = P_{g0}(\rho/\rho_0)^{5/3}.$$

Noting also that  $\rho u = \rho_0 V_s$  in the preshock, we obtain a relationship between the total Mach number  $M = V_s/c_{s0}$  and the local Mach number  $M_1$ ,

$$M_1 = M(\rho_1/\rho_0)^{-4/3},$$

whence the compression of matter in the preshock is

$$\rho_1/\rho_0 = (M/M_1)^{3/4} \quad (37)$$

and the total compression is

$$\sigma = \sigma_s (M/M_1)^{3/4}. \quad (38)$$

Equations (36)–(38) are in good agreement with the numerical results shown in Figs. 11 and 12.

A natural question arises: what basic physical principle makes such high compression in a shock wave possible, as predicted by Eq. (38) at high Mach numbers? To address this important question, we begin with the generalized Rankine–Hugoniot jump conditions, which can be obtained by integrating Eqs. (1)–(4) over  $r$  from  $R_s - 0$  to  $\infty$  to yield

$$\rho_2 u_2 = \rho_0 u_0 - j_e,$$

$$\rho_2 u_2^2 + P_2 = \rho_0 u_0^2 + P_{g0} - q_e,$$

$$\frac{\rho_2 u_2^3}{2} + u_2 \frac{\gamma_2}{\gamma_2 - 1} P_2 = \frac{\rho_0 u_0^3}{2} + u_0 \frac{\gamma_g}{\gamma_g - 1} P_{g0} - F_e.$$

These relations differ from the customary Rankine–Hugoniot jump conditions due to the presence of additional terms (mass, momentum, and energy flux, respectively):

$$j_e = j'_e \rho_0 u_0 = \int_{R_s}^{\infty} dr \left( \frac{2\rho w}{r} + \frac{\partial \rho}{\partial t} \right),$$

$$q_e = q'_e \rho_0 u_0^2 = \int_{R_s}^{\infty} dr \left( \frac{2\rho u w}{r} + \frac{\partial \rho u}{\partial t} \right),$$

$$F_e = F'_e \rho_0 u_0^3 = \int_{R_s}^{\infty} dr \left( \frac{2F}{r} + \frac{\partial E}{\partial t} \right) - F_{D2} + u_0 q_e - \frac{u_0^2 j_e}{2}.$$

In these equations,  $F$  is the energy flux density,  $E$  is the energy density, and  $F_{D2}$  is the diffusive flux of cosmic ray energy at the point  $r=R_s-0$ .

Solving the algebraic equations above, we obtain an expression for the total compression  $\sigma = \rho_2/\rho_0$ :

$$\sigma = \frac{\gamma_2 + 1}{\gamma_2 - 1} \times \frac{1 + j'_e(\gamma_g - 1)/2}{1 + \gamma_2 q'_e + (\gamma_g + \gamma_2)/[\gamma_g(\gamma_2 - 1)M^2] - (\gamma_2 + 1)F'_e}. \quad (39)$$

We see that the total compression can be expressed as a product of two factors. The first,  $(\gamma_2 + 1)/(\gamma_2 - 1)$ , yields the usual value for the compression of matter in an infinitely thin shock front, expressed in terms of the adiabatic index  $\gamma_2$  of the postshock medium. For an ionized monatomic gas,  $\gamma_2 = 5/3$ , which yields  $\sigma = 4$ . When cosmic rays are present, the effective adiabatic index of the medium (consisting of gas plus cosmic rays) can be close to  $4/3$ , yielding  $\sigma = 7$ .

The second factor in Eq. (39) can significantly increase the compression. In a strong shock ( $M \gg 1$ ), this factor differs from unity due to the nonvanishing fluxes  $j'_e$ ,  $q'_e$ , and  $F'_e$ . These describe the way in which the region encompassed by a spherical nonstationary shock front of finite thickness acts as a sink for fluxes of mass, momentum, and energy that are filling it. By virtue of the region's being a sink, the outgoing and incoming fluxes are unequal. Furthermore, the term  $F_{D2}$  in the expression for  $F_e$  indicates that the cosmic ray distribution immediately behind the shock can be nonuniform. The associated diffusive flux  $F_{D2}$ , if it is negative (i.e., directed toward the region with  $r < R_s$ ), results in energy being drained from the vicinity of the shock front (radiative losses), which, as in a traditional shock with such losses, is accompanied by increasing compression.

It can easily be seen that as the thickness of the shock front tends to zero, in which limit  $w$ ,  $F$ , and the time derivatives are all nonvanishing, the fluxes  $j_e$ ,  $q_e$ , and  $F_e + F_{D2}$  all vanish. It can be shown that the energy  $F_e$  plays the principal role in Eq. (39). Despite the preshock thickness being small compared to the size of the shock, as shown above,  $F_e$  is nonnegligible. To convince oneself of this, it suffices to evaluate just one term in the expression for  $F_e$ , namely the one associated with the diffusive flux of cosmic ray energy in the preshock:

$$F_D(r) = -\bar{\kappa} \frac{\partial E_c}{\partial r}.$$

Here  $E_c$  is the cosmic ray energy density and  $\bar{\kappa}(r)$  is the (spectral) mean diffusion coefficient. In a substantially modified wave, most of the cosmic ray energy is concentrated in the spectral range near the cutoff momentum  $p_m$  (see Fig. 2). This is in fact why the mean diffusion coefficient  $\bar{\kappa}$  over most of the preshock is close to  $\kappa(p_m)$ . We can therefore write

$$\int_{R_s}^{\infty} dr \frac{2F_D}{r} \approx \frac{2}{R_s} \int_{R_s}^{\infty} dr F_D \approx \frac{2\kappa(p_m)}{R_s} E_{c1},$$

where  $E_{c1}$  is the cosmic ray energy density at the thermal shock. Writing out the quantities that appear here as  $E_{c1} = k\rho_0 V_s^2$  and  $\kappa(p_m) = R_s V_s / K$  [see (24)], we obtain  $F'_e = 2k/K$ . In the free expansion stage  $K=6$ , and  $k$  is close to unity for a strongly modified wave. Hence, we estimate the flux to be  $F'_e \approx 0.3$ . It is clear from (39) that this value of the flux results in a substantial rise in the degree of compression.

We thus conclude that the basic physical reason for the rise in compression in a shock that efficiently accelerates cosmic rays is the dilution of a substantial fraction of the energy within the shock transition region, which in this regard is not thin. What is important here is that the very highest-energy cosmic rays are the principal players in this process, as they exhibit the greatest diffusion length and carry the brunt of the cosmic ray energy.

The expenditure of energy needed to fill a growing shock front of finite thickness has consequences similar to those produced by the extraction (radiative loss) of a fraction of the system's energy. It would seem that this is the very reason that the plane-wave description, which involves the cutoff momentum  $p_m$  as a parameter and takes account of the energy flux carried off from the system by particles that have reached  $p_m$ ,<sup>20,35</sup> qualitatively reproduces the behavior of the acceleration efficiency and the degree to which the shock has been modified, both as functions of the injection rate and the Mach number. In that regard, the arguments of Achterberg *et al.*<sup>42</sup> that a simplified description of cosmic ray acceleration that makes no use of information about the cutoff momentum  $p_m$  is of limited applicability would appear to be justified.

From somewhat of a different perspective, Eqs. (35)–(38) elucidate the reasons for the extremely high compression in a strong shock with Mach number  $M \gg 1$ , in which cosmic ray acceleration proceeds in the saturated regime. Specifically, Eq. (38) predicts an unbounded increase in compression with increasing  $M$ , and for a simple reason. The onset of stabilizing negative feedback under saturated acceleration conditions requires that compression in the thermal shock drop to the value given by Eq. (35). For this to happen, the local Mach number  $M_1$  must be reduced, which is accomplished by heating the gas via adiabatic compression in the preshock. Higher Mach numbers  $M$  require higher and higher compression of the preshock. One might say that the strong dependence  $\sigma \propto M^{3/4}$  described by (38) results from the low efficiency of adiabatic heating of the preshock.

### 3.8. Dissipation of Alfvén waves

Alternative mechanisms for heating the preshock can play an important role in this situation. Above all, heating of the gas in the preshock beyond that provided by adiabatic compression can result from the dissipation of Alfvén waves generated by cosmic ray particles. A systematic treatment of this mechanism must consider the dynamics of Alfvén turbulence, including wave damping. We can describe a frequently used simplified approach to this problem, which we adopt here, as follows.<sup>12,43</sup> Alfvén waves generated by cosmic ray particles at  $r > R_s$  rapidly reach their limiting amplitude

$\delta B \sim B_0$ , thus ensuring Bohm diffusion of the cosmic rays. Nonlinear damping mechanisms prevent any subsequent growth in the wave amplitude. Here, regardless of the details of the damping mechanism, the rate at which the gas is heated is exactly equal to the rate at which energy is transferred from cosmic rays to Alfvén waves.

Instead of (4), the gas pressure is then governed by the equation<sup>43</sup>

$$\frac{d}{dt}(P_g \rho^{-\gamma_g}) = (1 - \gamma_g) c_a \frac{\partial P_c}{\partial r} \rho^{-\gamma_g}, \quad (40)$$

where  $d/dt = \partial/\partial t + w \partial/\partial r$  and  $c_a = B/\sqrt{4\pi\rho}$  is the Alfvén velocity. Furthermore, since Alfvén waves in the preshock propagate primarily in the radial direction,  $w + c_a$  must be used at  $r > R_s$  in the transport equation (1) instead of the gas velocity. We can neglect dissipation in the postshock region, at  $r < R_s$ , primarily because the energy in Alfvén waves is low there relative to the gas energy.

Numerical calculations allowing for Alfvén wave dissipation in the preshock are plotted in Fig. 11 for an injection rate  $\eta = 10^{-3}$ , and in Fig. 12 for Mach numbers  $M_0 = 33$  (hot phase of the interstellar medium) and  $M_0 = 330$  (warm phase of the interstellar medium). Above all, it is clear from these figures that allowance for wave dissipation, which ensures more efficient gas heating in the preshock, lowers the cosmic-ray acceleration efficiency due to an appreciable decrease in the total compression  $\sigma$ . As before, the magnitude of  $\sigma$  is a rising function of  $\eta$  and  $M_0$ , but when both  $M_0$  and the injection rate increase, the compression reaches a limit (saturates) at  $\sigma \approx 7.3$ . The efficiency of cosmic ray acceleration then remains high: the cosmic ray energy  $E_c$  comprises approximately 50% of the overall explosion energy  $E_{SN}$ .

An analysis of the derivation of (35) for the compression at the thermal shock shows that it ought to hold even when Alfvén wave dissipation is present, which is consistent with the numerical results shown in Figs. 11 and 12. Making use of (40), Eq. (37) for the preshock compression takes the form

$$\frac{\rho_1}{\rho_0} = \left\{ \left( \frac{M_1}{M} \right)^2 + \frac{2}{3} M_1^2 \frac{c_a}{V_s} \left[ 1 - \left( \frac{\rho_0}{\rho_1} \right)^{5/3} \right] \right\}^{-3/8}. \quad (41)$$

This is consistent with Eq. (37) if we take  $c_a = 0$ . On the other hand, if  $c_a/V_s \gg 1/M^2$ , the preshock compression becomes essentially independent of the Mach number  $M$ . In the present case  $c_a \approx 100$  km/s and  $V_s = 5000$  km/s, and preshock heating becomes especially significant at Mach numbers  $M \gg \sqrt{50}$ , which is also in agreement with the calculations (Fig. 11).

Our main conclusion from the calculations is that the inclusion, over and above adiabatic compression, of additional mechanisms for heating the preshock—one of which might be the dissipation of Alfvén waves—substantially affects the evolution of the shock wave and the acceleration process. The properties of the modified shock and the cosmic-ray acceleration process become universal, to a large extent: the degree of modification of the shock wave and the efficiency of acceleration depend little on either the initial Mach number or the assumed injection rate, as long as  $M_0 > 10$  and  $\eta > 10^{-4}$ , which, in our opinion, is usually the case.

Note also that a simplified description of shock and cosmic ray dynamics<sup>12</sup> leads to the opposite result: the dissipation of Alfvén waves plays no appreciable role, except at the very latest stages of evolution ( $t > 10t_0$ ). We can ascribe this difference to the shortcomings of a hydrodynamic description of cosmic rays, at least in the form that one usually encounters. As noted above, we expect the two-fluid hydrodynamic description to be extremely sensitive to the choice of input parameter—the cosmic ray diffusion coefficient  $\bar{\kappa}(r, t)$ . The mere inclusion of time dependence<sup>40</sup> in  $\bar{\kappa}(t)$  fundamentally alters the results obtained with this theory, as compared with the results obtained with a coefficient  $\bar{\kappa}$  that is constant in time.<sup>39</sup> We believe the spatial dependence of  $\bar{\kappa}$  in the preshock region to be even more important. Moreover, it is still an open question as to whether one can accurately assess the behavior of the diffusion coefficient  $\bar{\kappa}(r, t)$  averaged over the cosmic ray spectrum without reconstructing the spectrum itself.

### 3.9. Post-shock pressure

The total internal pressure behind a strong shock front can be obtained from the relation

$$P_2 + \rho_2 u_1^2 = P_{g0} + \rho_0 V_s^2 - q_e$$

(see Sec. 3.7) if we neglect  $P_{g0}$  and  $q_e$ , which yields

$$P_2 = \rho_0 V_s^2 (\sigma - 1) / \sigma. \quad (42)$$

Similarly, the relation

$$P_{g2} + \rho_2 u_2^2 = P_{g1} + \rho_1 u_1^2$$

for a thermal shock with the cosmic-ray pressure ( $P_c$ ) discontinuity taken into consideration can be used to determine the postshock gas pressure  $P_{g2}$ . Since the Mach number is high for the thermal shock ( $M_1^2 \gg 1$ ),  $P_{g1}$  is negligible relative to  $\rho_1 u_1^2$ , which yields

$$P_{g2} = \rho_0 V_s^2 (\sigma_s - 1) / \sigma \quad (43)$$

when allowance is made for the conservation of the flux of matter ( $\rho_1 u_1 = \rho_0 V_s$ ) at the preshock.

We obtain from Eqs. (42) and (43) an expression for the cosmic ray pressure at the shock front:

$$P_{c2} = P_{c1} = \rho_0 V_s^2 (\sigma - \sigma_s) / \sigma. \quad (44)$$

This demonstrates that in the saturated acceleration regime, the ratio of the cosmic ray pressure to the dynamical pressure,  $P_{c1}/\rho_0 V_s^2 = 1 - \sigma_s/\sigma$ , is an increasing function of the Mach number  $M$ , in agreement with the calculations [Figs. 11 and 12]. At the same time, the postshock gas pressure  $P_{g2}/\rho_0 V_s^2 \propto M^{-3/4}$  becomes relatively low at high Mach numbers.

When allowance is made for dissipation of Alfvén waves in the preshock of a strong shock wave ( $M \gg 7$ ),  $\sigma_s \approx 3.5$  and  $\sigma \approx 7.3$ , which according to Eq. (43) and (44) yields  $P_{c2}/\rho_0 V_s^2 \approx 0.5$  and  $P_{g2}/\rho_0 V_s^2 \approx 0.3$ , regardless of the value of  $M$  and in good agreement with the calculations. Even though cosmic rays significantly modify the shock in this

case, the pressure and temperature of the postshock gas remain high, as required by x-ray observations of young supernova remnants.<sup>46</sup>

### 3.10. Cosmic ray penetration of ejecta

We now attempt to assess the extent to which various assumptions about the interaction between cosmic rays and the piston affect the final result. Recall that all results discussed above were obtained assuming a piston that was impenetrable to cosmic rays, corresponding to the boundary condition (15). Let us consider an alternative model that allows for the possibility of diffusive penetration of the piston by cosmic rays.

As before, we assume that matter in the piston is concentrated within a fairly thin shell of thickness

$$l_p = \delta R_p, \quad (45)$$

( $\delta \ll 1$ ). Retaining the assumed relationship (21) between the cosmic ray diffusion coefficient and the density of matter, we find that the distribution of cosmic rays traversing the thin shell of the piston into the region  $r < R_p$  can be taken to be uniform, since the cosmic ray diffusion coefficient here is fairly large, due to the low density of matter. In place of (1), we can then write the cosmic ray distribution function at  $r < R_p$  in the simpler form

$$\frac{\partial f}{\partial t} = \frac{V_p}{R_p} p \frac{\partial f}{\partial p} - \frac{S}{V} \Phi, \quad (46)$$

which allows for the adiabatic change in cosmic ray energy within the varying volume  $V = 4\pi R_p^3/3$ , and for the existence of a diffusive cosmic ray flux  $F_D = 4\pi p^2 \Phi$  through the surface bounding that volume,  $S = 4\pi R_p^2$ . Given the small thickness  $l_p$  of the piston, we can write for this diffusive flux

$$\Phi = -\frac{\kappa_p}{l_p} [f(r=R_p+0, p, t) - f(r=R_p-0, p, t)], \quad (47)$$

in which

$$\kappa_p = \kappa_0 \frac{\rho_0}{\rho_p} \quad (48)$$

is the cosmic ray diffusion coefficient in the piston, and

$$\rho_p = M_{ej}/V \quad (49)$$

is the mean density of the piston, which occupies a volume  $V = 4\pi R_p^2 l_p$ .

Note that we have assumed a piston of vanishing thickness in Eqs. (46) and (47), while in calculating the mean density of matter  $\rho_p$  we have assumed a finite thickness  $l_p$ . This is not a serious problem so long as  $l_p \ll R_p$ .

The possibility of diffusive leakage of cosmic rays through the piston also requires a change in the boundary condition (15) for the cosmic ray distribution function in the range  $R_p \leq r \leq R_s$ :

$$\kappa \frac{\partial f}{\partial r} = -\Phi \quad \text{for } r = R_p + 0. \quad (50)$$

Figures 11 and 12 show the results of calculations that allow for cosmic ray penetration of a piston with  $\delta = 0.1$  in

the hot phase of the interstellar medium ( $M_0 = 33$ ) at injection rates  $\eta = 10^{-4}$  and  $\eta = 10^{-3}$ . Clearly diffusion does not substantially affect cosmic ray acceleration or shock evolution: including it produces only a minor change (at most 5%) in the basic characteristics.

This result can be easily understood. In the early stages of evolution ( $t \ll t_0$ ), cosmic ray diffusion through the piston is slow due to the high density  $\rho_p \gg \rho_0$ , by virtue of which  $\kappa_p(p) \ll \kappa_0(p)$ .

In the late stages ( $t \gg t_0$ ), diffusion is also unimportant, but for a different reason—the volume enclosed within the region  $r < R_p$  is small compared to the overall volume occupied by cosmic ray particles ( $\sim 4\pi R_s^2/3$ ), since  $R_s \gg R_p$ . The filling of that small a volume with cosmic ray particles has little effect on their dynamics.

Naturally, the actual processes transpiring in the supernova ejecta (piston) are much more complicated than we have described here. We have ignored the existence of a reverse shock, which heats the matter in the shell and accelerates cosmic rays. But for the same general reasons, we believe that from the standpoint of the production (acceleration) of cosmic rays and the degree to which those cosmic rays influence the global properties of the system, these additional features can be neglected.

### 3.11. Chemical composition of cosmic rays

We now turn to one of the most important questions of all, which has recently riveted the attention of more and more researchers concerned with the origin of cosmic rays, namely their chemical composition. In this section, we present only preliminary results bearing on this complex and interesting question, which indicate that in principle, the theory of regular acceleration of cosmic rays in supernova remnants is capable of accounting for the observed composition of cosmic rays in the energy range  $\varepsilon \leq 10^{15}$  eV.

In considering the chemical composition of cosmic rays accelerated by a shock, the question of the mechanism of injection into the acceleration regime must be framed with some care. Thus far, as we have dealt solely with the fundamental constituent of cosmic rays—protons—the injection problem has entailed few subtleties. Indeed, as we have shown above, due to the self-regulating nature of the acceleration process, it turns out to be insensitive to the injection rate over a wide range ( $\eta > \eta_*$ ). Since both measurements of the interplanetary medium<sup>21</sup> and numerical modeling of a collisionless shock<sup>22</sup> suggest that an injection rate  $\eta \sim 10^{-3}$  is much higher than the critical rate, the theory makes predictions that are essentially independent of the details of the assumed injection mechanism.

When the question bears on the chemical composition of cosmic rays, however, the universality of the theoretical predictions (i.e., the extent to which the predictions are independent of  $\eta$ ) is considerably diminished. Atomic nuclei heavier than hydrogen are but a minor constituent of the interstellar medium, and therefore when such elements are accelerated by a shock wave, they do not exert a significant back influence. This then means that the ratio of protons to heavy nuclei in cosmic rays is directly proportional to their relative

injection rates. In order to correctly reconstruct the chemical composition of accelerated cosmic rays, it is necessary to know how the injection rate depends on the mass and charge of the particles.

Since there is presently no detailed theory of the injection mechanism, we will attempt to determine the mass- and charge-dependence of the particle injection rate in the acceleration regime on the basis of general considerations.

Charged-particle motion in a collisionless shock is governed by particle interactions with electromagnetic fields. The intensity of this interaction—in particular, the mean free path between scattering events—is therefore a function of the rigidity  $R=pc/Ze$  or the mass-to-charge ratio  $A/Z$ . The rigidity of protons is less than that of heavy ions with the same velocity. The thermal shock is therefore more transparent to cold ions crossing for the first time than it is to cold protons, and we would expect the postshock thermal distribution of ions to have the same characteristic thermal velocity as the proton distribution.

It would also be natural to suppose that the injection mechanism differentiates between particles according to their rigidity: only particles whose rigidity is above some critical value should be capable of crossing in the second time the thermal shock and being accelerated. Since the postshock thermal distribution of ions has high mean rigidity, we expect them to be injected preferentially over protons.

This can all be expressed mathematically:

$$p_{\text{inj}}^A = A p_{\text{inj}}, \quad \eta_A = \eta \frac{a_A}{a} e\left(\frac{A}{Z}\right), \quad (51)$$

where  $a$  is the mean number density (prevalence) of nuclei in the Galaxy, quantities with subscript  $A$  pertain to ions with mass number  $A$ , and unsubscripted quantities pertain to protons. The function  $e$  describes preferential injection of heavy ions, with

$$e(1) = 1, \quad e(x > 1) > 1.$$

For definiteness, we assume a power law:

$$e(x) = x^\beta, \quad \beta > 1.$$

The exponent  $\beta$  is a free parameter of our theory, and is chosen to reproduce the observed chemical composition of cosmic rays.

In comparing the calculated spectrum of cosmic rays produced by a supernova shock with the cosmic ray spectrum observed at the Earth, it must be borne in mind that they are related by

$$J(\varepsilon_k) \propto \tau_e(R) N(\varepsilon_k), \quad (52)$$

in which  $J(\varepsilon_k)$  is the intensity of cosmic rays with kinetic energy  $\varepsilon_k$  observed at the Earth,  $N(\varepsilon_k)$  is the energy spectrum of cosmic rays (the differential number density) produced in supernova remnants over their full course of evolution, and  $\tau_e$  is the mean lifetime of Galactic cosmic rays, which is a function of their rigidity  $R(\varepsilon_k)$  (see, for instance, Ref. 29). The shape of the cosmic ray spectrum  $N(\varepsilon_k)$  produced at the source differs from the shape of the observed spectrum  $J(\varepsilon_k)$ , as the lifetime  $\tau_e$  of a Galactic cosmic ray depends heavily on its energy (or more precisely, its rigid-

ity). The function  $\tau_e(R)$ , determined from the measured relationship between the primary (produced at the source) and secondary (produced by interactions between primary cosmic rays and nuclei in the interstellar medium) components of cosmic rays, is a power law:

$$\tau_e \propto R^{-\mu}, \quad \mu > 0. \quad (53)$$

Apart from protons, we have also considered He nuclei and nuclei in the CNO group, the Ne, Mg, Si group, and Ar–Ni (the iron group), for which the high-energy cosmic ray intensity has been measured. Expressing the prevalence of these groups in units of the hydrogen prevalence  $a$  at the cosmic ray source (in the interstellar medium), we have (see, e.g., Ref. 29)

$$a(\text{He}) = 0.1, \quad a(\text{C,N,O}) = 1.42 \cdot 10^{-3},$$

$$a(\text{Ne,Mg,Si}) = 1.8 \cdot 10^{-4}, \quad a(\text{Ar-Ni}) = 3.3 \cdot 10^{-5}.$$

The charge numbers  $Z$  of the ions are determined by the temperature of the interstellar medium. In the hot phase ( $T_0 = 10^6$  K), all of the ion types noted above are essentially fully ionized, in contrast to the warm interstellar medium ( $T_0 = 10^4$  K), where the temperature is not high enough. The initial equilibrium ionic charge is less than the nuclear charge, and can be calculated using the Saha equation. The mean charge and mass numbers  $Z$  and  $A$  are then determined for each of the above groups of nuclei, with their prevalence folded into the calculation.

In accordance with our adopted proton diffusion coefficient (20), (21), we have for ions with charge number  $Z$

$$\kappa_0(p, Z) = \kappa_0(p)/Z,$$

in which  $\kappa_0(p)$  is the proton diffusion coefficient in the undisturbed interstellar medium.

In Figs. 13 and 14, we compare the calculated spectra  $J(\varepsilon_k)$  for the five groups of nuclei cited above to the existing experimental data. The calculations correspond to the warm phase of the interstellar medium ( $T_0 = 10^4$  K, initial Mach number  $M_0 = 330$ ) and a moderate proton injection rate  $\eta = 2 \cdot 10^{-5}$ , with dissipation of Alfvén waves. The cosmic ray intensity given by Eq. (52) has been normalized so as to give the best fit to the observed proton spectrum in the energy range  $\varepsilon_k < 10^{14}$  eV. Under these same considerations, we have chosen a value for  $\mu$ , which specifies the dependence of Galactic cosmic ray lifetime (53) on rigidity. The calculations shown in the figures correspond to  $\mu = 0.75$ . Comparing this with the experimentally dictated requirements ( $\mu = 0.3-0.7$ ; see, e.g., Ref. 29), we find that the required value 0.75 is somewhat high. It must be borne in mind, however, that even a slight random preacceleration of cosmic rays in the postshock region, the possibility of which we have ignored, can soften the spectrum somewhat, leading to a reduction in the required value of  $\mu$ .

We obtain agreement with the experimental data for heavy nuclei with an enrichment factor  $e = (A/Z)^{0.8}$  [see Eq. (51)]. Note that the degree of ionization (i.e., our required charge number  $Z$ ) can vary (increase) as acceleration proceeds, something that we have also not considered. Since the acceleration time of cosmic rays corresponding to the

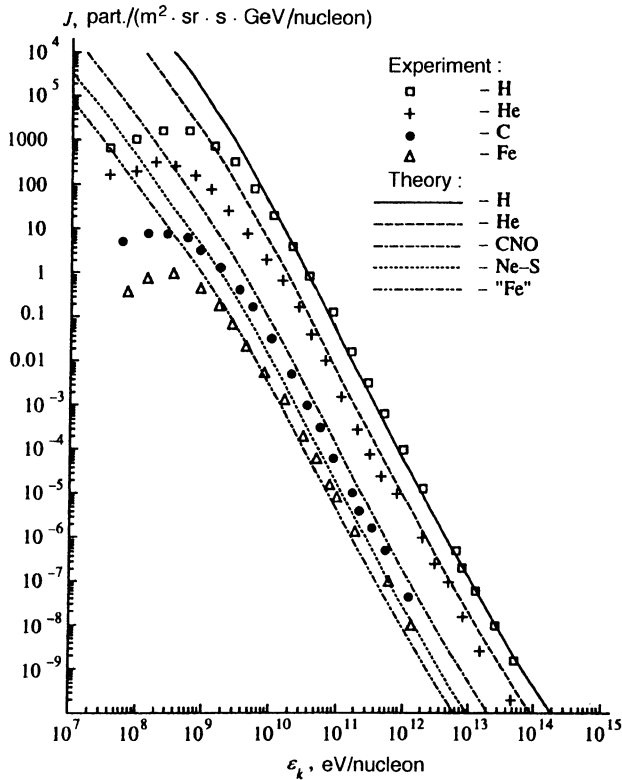


FIG. 13. Energy spectrum of various chemical constituents of Galactic cosmic rays. Experimental values are taken from Ref. 44. Calculations assumed an initial Mach number  $M_0 = 330$  and proton injection rate  $\eta = 2 \cdot 10^{-5}$ , and allowed for dissipation of Alfvén waves. The injection rate of heavy nuclei is given by (51).

adopted diffusion coefficient (20) grows with increasing energy, a change in the charge of the ions can affect their spectrum at the highest energies.

We must also note that at energies  $\lesssim 10$  GeV/nucleon, the shape of the observed cosmic ray spectrum can be modulated by the solar wind, so direct comparison of theory with experiment is only possible at energies  $\gtrsim 10$  GeV/nucleon. Thus, a comparison of computed results with direct measurements<sup>44</sup> (Fig. 13) indicates satisfactory agreement for all types of nuclei if we bear in mind that one-third of the arriving CNO nuclei are carbon, due to its prevalence, and that the most prevalent element in the Ar–Ni group is iron.

The same calculations (with the same normalization) are compared in Fig. 14 over a wider energy range with experimental data from HEAO and Spacelab 2, from balloon experiments (JACEE), and from measurements of the total cosmic ray intensity.<sup>45</sup>

Here it is clear that the theory fits the total cosmic ray intensity quite well up to  $\sim 10^{15}$  eV, and it is also in satisfactory agreement with existing measurements of the spectra of the various groups of constituent nuclei. Ignoring the fact that we are dealing with small-number statistics, we point out somewhat of a discrepancy between theory and experiment at the very highest energies,  $\epsilon_k \gtrsim 10^{14}$  eV. According to the measurements, the proton spectrum begins to steepen at  $\epsilon_k \approx 10^{14}$  eV, while the heavy-element spectra tend to harden at  $\epsilon_k \gtrsim 10^{14}$  eV. This trend becomes all the more prominent among the heaviest of the groups.

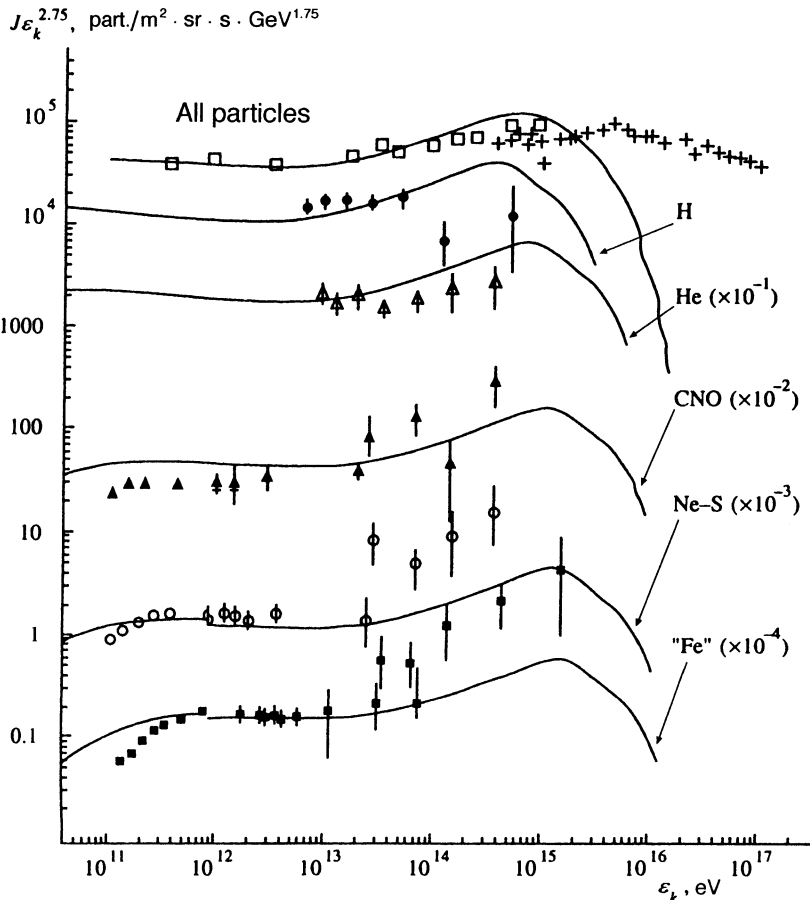


FIG. 14. Energy spectrum of various chemical constituents of Galactic cosmic rays. Experimental values are taken from Ref. 45. Computed results are the same as in Fig. 13.

The theory also reproduces the fact that the spectrum hardens in the energy range  $10^{13}$ – $10^{15}$  eV, but not so strongly as it does observationally. The most difficult thing to explain theoretically is the great variety among the spectra of protons and heavy elements at  $\varepsilon_k > 10^{14}$  eV. Conceivably, if we drop our assumption about interaction between the magnetic field and the density of matter ( $B_0 \propto \sqrt{\rho_0}$ ) and instead employ the same field as in the hot interstellar medium,  $B_0 = 3 \mu\text{G}$ , the peak energy of protons accelerated in supernova remnants falls by an order of magnitude to  $10^{14}$  eV. The limiting energy of heavy nuclei is a factor of  $Z$  higher. Thus, if we entertain the possibility of nuclei becoming fully ionized via acceleration, an iron nucleus will be accelerated to  $\sim 3 \cdot 10^{15}$  eV.

One remaining problem of no small import is the elucidation of the contribution of the various phases of the interstellar medium to the observed spectrum of cosmic rays.

More detailed calculations to be completed in the near future and higher-precision measurements of the chemical composition of cosmic rays in the  $10^{14}$ – $10^{16}$  eV energy range<sup>45,46</sup> should make it possible to estimate the highest energies in the observable spectrum of cosmic rays produced in supernova remnants.

#### 4. CONCLUSION

The principal distinction between the results presented in the present paper and previous investigations<sup>13</sup> is that we have considered for the first time and studied in detail the evolution of a supernova remnant and cosmic ray acceleration with allowance for the energy dependence of the diffusion coefficient, which provides for the efficient acceleration of cosmic rays and substantial modification of the shock.

We have established that precisely in the case in which nonlinear interactions between cosmic rays and the medium are significant, the spherical shock produced by the supernova evolves in a manner that is fundamentally different from that predicted on the basis of the plane-wave approximation or simplified models. Geometrical factors such as the finite size of the shock and the increasing volume of the preshock lead to a situation in which the shock cannot be completely altered by cosmic ray pressure: the thermal shock does not disappear, but instead plays an important role in the dynamics of cosmic ray acceleration and shock evolution.

In the absence of nonadiabatic mechanisms that heat the preshock, the compression  $\sigma_s$  of the thermal shock is given by (35), which reproduces the weak (logarithmic) dependence of  $\sigma_s$  on the Mach number  $M$  and the injection rate. For reasonable values of the parameters that enter into (35), the compression of the thermal shock in a strong shock wave ( $M \geq 10$ ) does not drop below 2.5, which is also confirmed by numerical calculations. Furthermore, during the rapid acceleration of cosmic rays by a strong shock ( $M > 10$ ), when the injection rate is above a critical value, the structure of the shock is greatly modified by cosmic ray pressure, with the degree of modification rising rapidly with increasing Mach number  $M$ . The total compression of matter in a shock, which characterizes the degree of modification ( $\sigma \propto M^{3/4}$ ), can be extremely high at large Mach numbers ( $\sigma \approx 77$  at

$M = 330$ ). The physical causes of high compression  $\sigma \gg 4$  include the dilution (distribution) of a substantial fraction of the energy in the preshock [see Eq. (39)], which in this respect is similar to a shock with radiative cooling.

Nonlinear effects due to the back influence of accelerated cosmic rays on the structure of the shock become significant only at a sufficiently high injection rate of suprathermal particles into the acceleration regime, with the injection rate exceeding a certain critical value  $\eta_*$  given by (33).

At  $\eta < \eta_*$ , the acceleration of cosmic rays is a linear (unsaturated) process. Cosmic ray energy and pressure at the shock front are proportional to the injection rate, and the degree of modification of the shock is small.

At high injection rates ( $\eta > \eta_*$ ), cosmic ray acceleration is saturated, and because of the self-regulating properties of the acceleration process, the efficiency of cosmic ray acceleration and the degree of shock modification are both high and largely independent of  $\eta$  as the latter ranges widely. This property was previously noted<sup>20</sup> during modeling of cosmic ray acceleration in the plane-wave approximation. Since the critical rate is low for typical parameters of supernovae and the interstellar medium, there is reason to believe that the actual particle injection rate in the acceleration regime is above critical. In that event, the predictions of the theory are largely independent of the specific value of this free parameter.

In the saturated injection regime, higher levels of compression are encountered in a strong shock due to the inadequate efficiency of adiabatic heating of the preshock. Under these circumstances, other possible gas heating mechanisms in the preshock become exceptionally important. One of these may be the dissipation of Alfvén waves generated by cosmic ray particles. Allowance for Alfvén wave dissipation significantly limits the extent to which a strong shock can be modified. In the saturated acceleration regime, the total compression of matter in a strong shock ( $M > 10$ ) is  $\sigma \approx 7.3$ , and depends only weakly on the parameters of the problem. The acceleration efficiency remains high. Approximately 50% of all the mechanical energy liberated in the blast ( $E_{SN}$ ) is transferred to cosmic ray particles. This is undoubtedly sufficient to cover the production of cosmic rays leaving the Galaxy (see, e.g., Ref. 29). In the postshock region of a strong shock ( $M \geq 10$ ), one-third of the thermal pressure comes from gas, and two-thirds from cosmic ray particles. In other words, the gas temperature behind a strong shock, despite being lower (by a factor of 2.5) than the temperature in a classical shock with no cosmic rays, remains high enough to be consistent with x-ray observations of supernova remnants.<sup>46</sup>

A comparison of our calculations with experimental data shows that the theory satisfactorily accounts for the observed cosmic ray spectrum up to energies of  $10^{14}$ – $10^{15}$  eV. With regard to chemical composition, theoretical predictions in this area depend strongly on the injection rate  $\eta$  of ions with different mass and charge numbers  $A$  and  $Z$ . The lack of a comprehensive theory for a collisionless quasiparallel thermal shock precludes an informed choice for the function  $\eta(A, Z)$ . We have shown that it is possible to satisfactorily

account for the existing experimental data on chemical composition up to  $10^{15}$  eV by making several assumptions—which we believe to be physically reasonable—about the ratio of injection rates among different types of particles. Nevertheless, a great deal more progress is required on both the theoretical and experimental fronts before we can come to any kind of well-founded conclusions relating to this important problem.

Besides a theoretical injection mechanism, we still lack a detailed description of Alfvén wave dynamics in the pre-shock. Neglect of the dynamics of Alfvén turbulence, as one finds in most work of this type, is based on energy considerations. In the vicinity of a strong shock front, cosmic rays carry far more energy than turbulence. Only a detailed description of turbulence, however, can tell us how broadly applicable the assumption of a Bohm diffusion coefficient is for cosmic rays near a shock front.

This work was carried out with financial support from the Russian Fund for Fundamental Research (Grant No. 93-02-02990). A significant portion of the work was completed during a visit by two of the authors (E. G. B. and L. T. K.) to the Max Planck Institute for Nuclear Physics in Heidelberg. The authors are sincerely grateful to H. J. Völk and G. F. Krymskiĭ for useful discussions throughout this work.

- <sup>1</sup>V. L. Ginzburg and S. I. Syrovatskiĭ, *The Origin of Cosmic Rays*, Nauka, Moscow (1963) [New York, Macmillan (1964)].
- <sup>2</sup>G. F. Krymskiĭ, Dokl. Akad. Nauk SSSR **234**, 1306 (1977) [Sov. Phys. Dokl. **22**, 327 (1977)].
- <sup>3</sup>W. I. Axford, E. Leer, and G. Skadron, in *Proc. 15th Int. Cosmic Ray Conf.*, Vol. 11, Plovdiv (1977), p. 132.
- <sup>4</sup>R. D. Blandford and J. R. Ostriker, *Astrophys. J.* **221**, 129 (1978).
- <sup>5</sup>L. O'C. Drury, *Rep. Progr. Phys.* **46**, 973 (1983).
- <sup>6</sup>E. G. Berezhko and G. F. Krymskiĭ, *Usp. Fiz. Nauk* **154**, 49 (1988) [Sov. Phys. Usp. **31**, 27 (1988)].
- <sup>7</sup>E. G. Berezhko, V. K. Elshin, G. F. Krymskiĭ, and S. I. Petukhov, *Shock-Wave Generation of Cosmic Rays*, [in Russian], Nauka, Novosibirsk (1988).
- <sup>8</sup>L. O'C. Drury and H. J. Völk, *Astrophys. J.* **298**, 344 (1981).
- <sup>9</sup>W. I. Axford, E. Leer, and J. F. McKenzie, *Astron. Astrophys.* **111**, 317 (1982).
- <sup>10</sup>H. Kang and T. W. Jones, *Astrophys. J.* **353**, 149 (1990).
- <sup>11</sup>L. O'C. Drury, H. J. Völk, and W. J. Markiewicz, *Astron. Astrophys.* **225**, 179 (1989).
- <sup>12</sup>W. J. Markiewicz, L. O'C. Drury, and H. J. Völk, *Astron. Astrophys.* **236**, 487 (1990).
- <sup>13</sup>H. Kang and T. W. Jones, *Mon. Not. R. Astron. Soc.* **249**, 439 (1991).

- <sup>14</sup>E. G. Berezhko, V. K. Elshin, and L. T. Ksenofontov, *Astropart. Phys.* **2**, 215 (1994).
- <sup>15</sup>E. F. Krymskiĭ, *Geomagn. Aëron.* **4**, 977 (1964).
- <sup>16</sup>I. N. Parker, *Planet. Space Sci.* **13**, 9 (1965).
- <sup>17</sup>E. G. Chernyi, Dokl. Akad. Nauk SSSR **112**, 113 (1957) [Sov. Phys. Dokl. (1957)] [*sic*].
- <sup>18</sup>D. C. Ellison, F. C. Jones, and D. Eichler, *J. Geophys.* **50**, 110 (1981).
- <sup>19</sup>G. F. Krymskiĭ, *Izv. Akad. Nauk SSSR, Ser. Fiz.* **45**, 461 (1981).
- <sup>20</sup>E. G. Berezhko, V. K. Elshin *et al.*, *Izv. Akad. Nauk SSSR, Ser. Fiz.* **45**, 461 (1981).
- <sup>21</sup>M. A. Lee, *J. Geophys. Res. A* **87**, 5063 (1982).
- <sup>22</sup>K. B. Quest, *J. Geophys. Res. A* **93**, 9649 (1988).
- <sup>23</sup>E. G. Berezhko, in *Proc. 24th Int. Cosmic Ray Conf.*, Vol. 3, Rome (1995), p. 372.
- <sup>24</sup>A. R. Bell, *Mon. Not. R. Astron. Soc.* **182**, 147 (1978).
- <sup>25</sup>E. G. Berezhko and S. N. Taneev, *Kosm. Issled.* **29**, 582 (1991).
- <sup>26</sup>L. O'C. Drury, *Adv. Space Res.* **4**, 185 (1984).
- <sup>27</sup>E. G. Berezhko, *Pis'ma Astron. Zh.* **12**, 842 (1986) [Sov. Astron. Lett. **12**, 352 (1986)].
- <sup>28</sup>E. G. Berezhko, in *Proc. Joint Varenna-Abastumani Int. School and Workshop on Plasma Astrophysics*, Suhumi (1986), ESA SP-251, p. 271.
- <sup>29</sup>V. S. Berezhinskiĭ *et al.*, *Cosmic Ray Astrophysics* [in Russian], Nauka, Moscow (1984).
- <sup>30</sup>P. Duffy, L. O'C. Drury, and H. J. Völk, *Astron. Astrophys.* **291**, 449 (1994).
- <sup>31</sup>H. Moraal and W. I. Axford, *Astron. Astrophys.* **125**, 204 (1983).
- <sup>32</sup>T. Y. Bogdan and H. J. Völk, *Astron. Astrophys.* **12**, 129 (1983).
- <sup>33</sup>A. E. Ammosov, E. G. Berezhko, and V. K. Elshin, *Astron. Zh.* **67**, 572 (1990) [Sov. Astron. **34**, 286 (1990)].
- <sup>34</sup>D. Eichler, *Astrophys. J.* **277**, 429 (1984).
- <sup>35</sup>D. C. Ellison and D. Eichler, *Astrophys. J.* **286**, 691 (1984).
- <sup>36</sup>G. F. Krymskiĭ, V. K. Elshin *et al.*, *Izv. Akad. Nauk SSSR, Ser. Fiz.* **42**, 1070 (1978).
- <sup>37</sup>W. I. Axford, in *Proc. Int. School and Workshop on Plasma Astrophysics*, Varenna (1981), ESA SP-161, p. 425.
- <sup>38</sup>L. O'C. Drury, H. J. Völk, and E. G. Berezhko, *Astron. Astrophys.* **299**, 222 (1995).
- <sup>39</sup>E. A. Dorfi, *Astron. Astrophys.* **234**, 419 (1990).
- <sup>40</sup>E. A. Dorfi, *Astron. Astrophys.* **235**, 597 (1992).
- <sup>41</sup>T. W. Jones and H. Kang, *Astrophys. J.* **356**, 575 (1992).
- <sup>42</sup>A. Achterberg, R. D. Blandford, and V. Periwal, *Astron. Astrophys.* **132**, 97 (1984).
- <sup>43</sup>J. F. McKenzie and H. J. Völk, *Astron. Astrophys.* **116**, 191 (1984).
- <sup>44</sup>J. A. Simpson, *Ann. Rev. Nucl. Part. Sci.* **33**, 323 (1983).
- <sup>45</sup>J. Waddington, M. Forman, T. Guisler *et al.*, *GOAL Proposal*, NASA Goddard Space Flight Center, Greenbelt, Maryland (1992).
- <sup>46</sup>G. Schatz, *Interdisciplinary Sci. Rev.* **18**, 306 (1993).
- <sup>47</sup>B. Aschenbach, in *Supernova Remnants and the Interstellar Medium*, IAU Colloq. No. 101, R. S. Roger and T. L. Landecker (eds.), Penticton, British Columbia, Cambridge University Press, New York (1988), p. 99.

Translated by Marc Damashek